Journal of Biomolecular Structure and Dynamics, 2014
Vol. 32, No. 9, 1456–1473, http://dx.doi.org/10.1080/07391102.2013.820110

Taylor & Francis
Taylor & Francis Group

Complex of the herpes simplex virus type 1 origin binding protein UL9 with DNA as a platform for the design of a new type of antiviral drugs

N.P. Bazhulina[a], A.N. Surovaya[a], Y.G. Gursky[b], V.L. Andronova[c], E.D. Moiseeva[a], A.M. Nikitin[a], M.V. Golovkin[a], G.A. Galegov[c], S.L. Grokhovsky[a] and G.V. Gursky[a]*

[a]*V.A. Engelhardt Institute of Molecular Biology, Russian Academy of Sciences, ul. Vavilova 32, 119991 Moscow, Russia;* [b]*Russian Cardiology Research-and-Production Complex, 3ya Cherepkovskaya ul. 15a, 121552 Moscow, Russia;* [c]*D.I.Ivanovsky Institute of Virology, Russian Ministry of Health Care and Social Development, ul. Gamalei 16, 123098 Moscow, Russia*

Communicated by Vsevolod Makeev

(*Received 5 December 2012; final version received 25 June 2013*)

The herpes simplex virus type 1 origin-binding protein, OBP, is a DNA helicase encoded by the UL9 gene. The protein binds in a sequence-specific manner to the viral origins of replication, two OriS sites and one OriL site. In order to search for efficient inhibitors of the OBP activity, we have obtained a recombinant origin-binding protein expressed in *Escherichia coli* cells. The UL9 gene has been amplified by PCR and inserted into a modified plasmid pET14 between NdeI and KpnI sites. The recombinant protein binds to Box I and Box II sequences and possesses helicase and ATPase activities. In the presence of ATP and viral protein ICP8 (single-strand DNA-binding protein), the initiator protein induces unwinding of the minimal OriS duplex (≈80 bp). The protein also binds to a single-stranded DNA (OriS*) containing a stable Box I-Box III hairpin and an unstable AT-rich hairpin at the 3′-end. In the present work, new minor groove binding ligands have been synthesized which are capable to inhibit the development of virus-induced cytopathic effect in cultured Vero cells. Studies on binding of these compounds to DNA and synthetic oligonucleotides have been performed by fluorescence methods, gel mobility shift analysis and footprinting assays. Footprinting studies have revealed that Pt-bis-netropsin and related molecules exhibit preferences for binding to the AT-spacer in OriS. The drugs stabilize structure of the AT-rich region and inhibit the fluctuation opening of AT-base pairs which is a prerequisite to unwinding of DNA by OBP. Kinetics of ATP-dependent unwinding of OriS in the presence and absence of netropsin derivatives have been studied by measuring the efficiency of Forster resonance energy transfer (FRET) between fluorophores attached to 5′- and 3′- ends of an oligonucleotide in the minimal OriS duplex. The results are consistent with the suggestion that OBP is the DNA Holiday junction (HJ) binding helicase. The protein induces conformation changes (bending and partial melting) of OriS duplexes and stimulates HJ formation in the absence of ATP. The antiviral activity of bis-netropsins is coupled with their ability to inhibit the fluctuation opening of AT base pairs in the A + T cluster and their capacity to stabilize the structure of the AT-rich hairpin in the single-stranded oligonucleotide corresponding to the upper chain in the minimal duplex OriS. The antiviral activities of bis-netropsins in cell culture and their therapeutic effects on HSV1-infected laboratory animals have been studied.

Keywords: herpes simplex virus type 1; replication origin binding protein; DNA helicase; FRET method; bis-linked netropsin derivatives; antiviral activity

Introduction

The use of therapeutically active chemical compounds able to bind selectively to viral DNA and to inhibit the activities of key viral DNA-binding proteins is one of the perspective approaches to therapy of the diseases caused by DNA-containing viruses. Nucleosides related to acyclovir are the only compound class available at present for systematic treatments of herpes disease. In the present work, new minor groove binding ligands have been synthesized which selectively inhibit development of virus-induced cytopathic effect in Vero cell culture infected with HSV1. In the past 20 years, great progress has been achieved in the design and synthesis of low-molecular-weight compounds that can bind to DNA at selected sites. Most of the synthesized sequence-specific DNA-binding compounds are derivatives of antitumor antibiotics netropsin and distamycin or dye Hoechst 33258 (for reviews see Bailly & Chaires, 1998). Studies on DNA-binding behavior of the antibiotics netropsin and distamycin have afforded a valuable insight into general mechanisms whereby small molecules can recognize target sites on DNA. X-ray (Coll,

*Corresponding author. Email: annasur@eimb.ru, gursky@eimb.ru

Frederick, Wang, & Rich, 1987; Kopka, Yoon, Goodsell, Pjura, & Dickerson, 1985), and NMR (Klevit, Wemmer, & Reid, 1986) studies have shown that these two antibiotics bind in the minor DNA groove at runs of four and five AT- base pairs. Their binding specificity derives from specific hydrogen bonding interactions between the amide NH groups of the antibiotic molecule and the thymine O2 and adenine N3 atoms, electrostatic interactions and van der Waals contacts with the floor and both sides of the minor groove. An obvious way to enhance the binding specificity shown by these antibiotics is to synthesize dimer compounds (bis-netropsins and bis-distamycins) in which two monomers are covalently linked by different linkers (Gursky et al., 1983; Khorlin et al., 1980; Lown, Krowicki, Balzarini, Newman, & De Clerk, 1989; Mrksich, Parks, & Dervan, 1994). NMR and X-ray studies also revealed that two distamycin (lexitropsin) molecules can be packed in an antiparallel side-by-side manner in the minor DNA groove (Chen, Ramakrishnan, Rao, & Sundaralingam, 1994; Geierstanger, Mrksich, Dervan, & Wemmer, 1994; Kopka et al., 1997; Pelton & Wemmer, 1989). Single-stranded and double-stranded pyrrole(imidazole) carboxamide motifs and conjugates of pyrrole carboxamides with peptides can be used to recognize a broad category of nucleotide sequences in the minor DNA groove (Geierstanger et al., 1994; Grokhovsky, Gottikh, & Zhuze 1992; Grokhovsky et al., 1988, 1993, 1998; Gursky et al., 2008; Janssen, Cuvier, Muller, & Laemmli, 2000; Kleikopf et al., 2000; Leinsoo et al. 1988; Meier, Montgomery, & Dervan, 2012; Nikolaev et al., 1996; Surovaya et al., 1995; White, Szewczyk, Turner, Baird, & Dervan, 1998). Such molecules could be expected to influence the binding of regulatory proteins to DNA and to act as potential regulators of gene expression. This has been demonstrated in prokaryotic and eukaryotic cells, with down-regulation of promoter activities in some cases (Belikov, Grokhovsky, Isaguliants, Surovaya, & Gursky, 2005; Coull et al., 2002; Dickinson et al., 1998; Gearhart et al., 2005; Gursky et al., 1983; Meier et al., 2012). Sequence-specific DNA-binding ligands can also be used to inhibit initiation of replication of viral DNA and to serve as potential antiviral drugs. In the present paper, we provide experimental evidence that complexes of the herpes simplex virus type 1 (HSV1) OBP with the viral replication origins, two OriS sites and one OriL site, serve as perspective targets for suppression of the diseases caused by HSV1. Previous studies showed that bis-linked netropsin derivatives effectively suppress development of virus-induced cytopathic effect in the cultured cells (Andronova et al., 2008; Andronova, Grokhovsky, Surovaya, Gursky, & Galegov, 2001, 2004; Lown et al., 1989). They also exert therapeutic effects on laboratory animals infected by HSV1 (Andronova et al., 2012; Andronova, Grokhovsky, Surovaya, Gursky, & Galegov, 2007).

Figure 1 shows the nucleotide sequence of the OriS and the hypothetical hairpin structures formed in the upper strand of the minimal duplex OriS (63 base pairs) after separation of DNA strands (Aslani, Macao, Simonsson, & Elias, 2001; Aslani, Olsson, & Elias, 2002; Bazhulina et al., 2012; Surovaya et al., 2010). In the present study, kinetics of DNA unwinding by OBP was monitored by measuring the efficiency of the resonance energy transfer between the fluorophore and quencher covalently linked to the 5′- and 3′-ends of the oligonucleotide. The data obtained suggest that Pt-bis-netropsin inhibits the unwinding of the OriS duplex by OBP. We investigated antiviral activities of bis-netropsins and their therapeutic effects on the HSV1-infected laboratory animals.

The efficiency of the resonance energy transfer between the fluorophore and quencher linked to the 5′- and 3′-ends of the oligonucleotide could be measured and used to estimate the distance between the fluorophore and the quencher. It is known that OBP is a multifunctional protein that initiates the unwinding of the replication origins in the presence of ATP and ICP8 (single-strand DNA-binding viral protein) (Aslani et al., 2001, 2002; Chattopadhyay & Weller, 2007; Fierer & Challberg, 1992; He & Lehman, 2001; Koff, Schwedes, & Tegtmeyer, 1991; Lee & Lehman, 1997; Macao, Olsson, & Elias, 2004; Malik & Weller, 1996; Olsson et al., 2009; Weir & Stow, 1990). The viral protein ICP8 forms a 1:1 complex with OBP and simulates ATP-dependent unwinding of DNA (Boehmer, Craigie, Stow, & Lehman, 1994; He & Lehman, 2001; Lee & Lehman, 1997; Manolaridis et al., 2009).

After unwinding of the OriS duplex, OBP binds to one of the single-stranded oligonucleotides (the upper strand in the minimal OriS duplex) (Aslani et al., 2001, 2002; Macao et al., 2004; Olsson et al., 2009). In solution, this oligonucleotide forms spontaneously two hairpins: a GC-rich hairpin stabilized by complementary base pairing of Boxes I and III, and an AT-rich hairpin which contains nucleotides in the A + T-rich segment and flanked regions (Aslani et al., 2002; Macao et al., 2004).

In the present studies, we used OBP and fluorescently labeled OriS DNA fragments. Prior to experiment, the HSV1 UL9 gene (strain L_2 from the State Virus Collection of D.I. Ivanovsky Institute of Virology) was amplified by PCR, inserted into plasmid pET14 and expressed in *E. coli* cells. The recombinant UL9 protein forms specific complexes with Boxes I and II in OriS and is endowed with helicase and ATPase activities (Bazhulina et al., 2012; Surovaya et al., 2010).

Materials and methods

Ligands

The chemical structures of netropsin and bis-netropsins used in the present work are displayed in Figure 2.

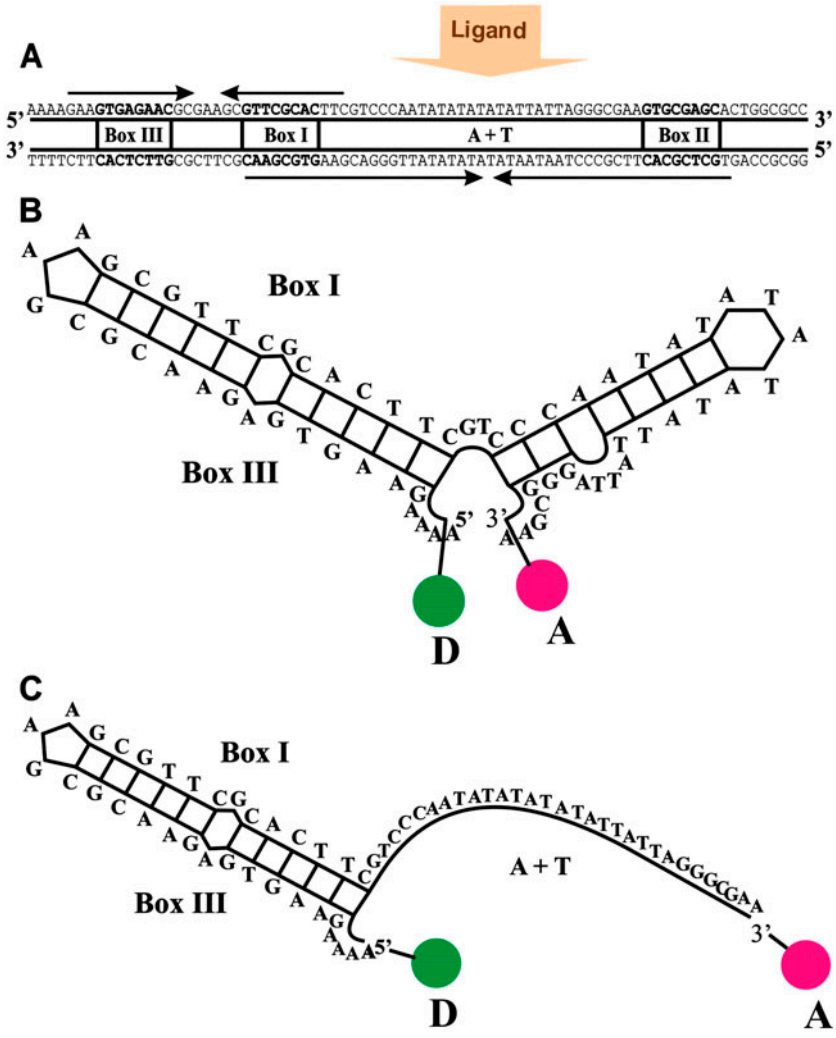

Figure 1. The nucleotide sequence at the HSV1 origin of replication OriS (A). The positions of DNA segments carrying palindromic sequences are indicated by arrows. These segments contain binding sites I and III for helicase (Boxes I and III), the A + T cluster and Box II. D and A – donor and acceptor molecules covalently linked to the 5′- and 3′-ends of the oligonucleotide in the minimal duplex OriS. Indicated are the proposed stem and loop structures for a fragment (63 nt) of the upper chain in the minimal OriS duplex (panels B and C).

Pt-bis-Nt and Pt*-bis-Nt contain a glycinated *cis*-diammino-platinum-group which bridges two netropsin-like fragments. 15Lys-bis-Nt and Lys-bis-Nt contain a triglycine and cadaverine residue, respectively, as a linker between two netropsin-like fragments. Synthesis of Pt-bis-Nt and related molecules were carried as described elsewhere (Grokhovsky et al., 1992). The main distinction of di-N-propyl pyrrolecarboxamide fragment of each bis-netropsin from the parent antibiotic netropsin (Nt) was that the N-methylpyrrole ring replaced N-propylpyrrole, the C-terminal amidine group of netropsin was replaced by the tertiary amine residue and the guanydylacetic acid residue was replaced by glycine residues. These replacements enhanced the stability of bis-linked netropsin derivatives in aqueous solutions. Concentrations of bis-linked netropsin were determined spectrophotometrically by using a molar extinction coefficient of 42,000 M^{-1} cm^{-1} at 297 nm.

Recombinant UL9 protein

The full-sized recombinant UL9 protein was synthesized on the basis of the modified plasmid PET14 carrying a HSV1 UL9 gene (strain L_2 from the State Virus Collection of D.I. Ivanovsky Institute of Virology) (Surovaya et al., 2010). The protein contains a histidine "tag", that is, a cluster of six N-terminal histidine residues enabling protein purification on metal-chelating (Ni-NTA) columns (Quiagen). Protein concentration was determined spectrophotometrically using a molar extinction coefficient for the UL9 monomer of 89,000 M^{-1} cm^{-1} at 280 nm (Surovaya et al., 2010). The recombinant protein was stored in the buffer containing 20 mM Tris HCl (pH

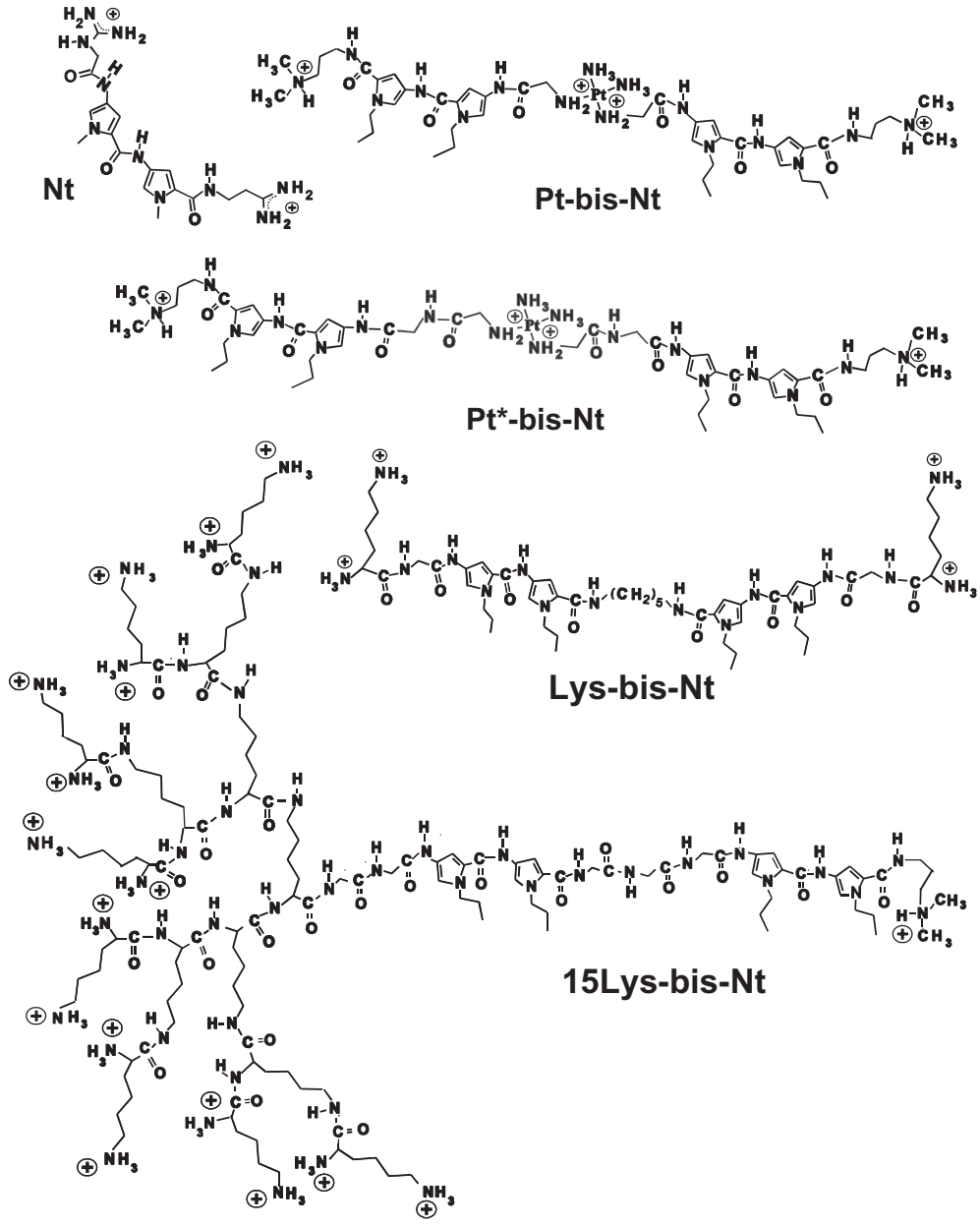

Figure 2. Chemical structures of netropsin (Nt) and bis-linked netropsin derivatives: Pt-bis-Nt, Pt*-bis-Nt, Lys-bis-Nt, and 15Lys-bis-Nt.

7.2), 20 mM HEPES-NaOH, .54 M NaCl, .01% Tween 20, .10 mM EDTA, 1 mM dithiothreitol and 20% (v/v) glycerol.

DNase I footprinting

The DNA fragment was obtained by cleavage of the modified plasmid pGEM7(f+) (Promega) carrying oligonucleotide inserts with pseudosymmetric sequences by restrictases NcoI and ApaI (Grokhovsky et al., 1998). In addition, the DNA fragment contained a segment of OriS DNA with the 5′-CTTCGCCCTAATAATATATATA-TATTGGGTCGAAGTGCGAACGC-3′ sequence carrying an A + T-rich segment and binding sites I and II for UL9 helicase. Radiolabelling at the 3′-end of this DNA fragment was carried out using [α-^{32}P]dATP (Izotop, Moscow), nonlabeled dNTP and the Klenow fragment of *E. coli* DNA polymerase I. The isolation procedure was performed in 5% polyacrylamide gel (Sambrook, Fritsch, & Maniatis, 1989). Footprinting of DNA complexes with bis-netropsins was performed using the previously described procedure (Grokhovsky et al., 1998). Briefly, 10 µl of the DNA solution ($\sim 10^4$ Bq) in 10 mM Tris-HCl

(pH 7.5) and .5 M NaCl pH 6.0 were mixed with 10 µl of the ligand solution in H_2O. After cooling to 0°C, 20 µl of the DNase I solution in 10 mM Tris-HCl (pH 6.0), .25 M NaCl and 5 mM $MnCl_2$ were added and the mixture was incubated for 3 min at 0°C. The reaction was stopped by adding 85 µl of a solution containing .15 M NaCl, 50 mM Tris-HCl (pH 7.5), 10 mM EDTA and 10 µg/ml tRNA. After phenol extraction and precipitation with ethanol, the DNA was washed with 70% ethanol, dried and dissolved in 1 µl of 95% formamide containing 15 mM EDTA, .05% bromphenol blue and .05% xylenecyanol FF. The resulting solution was heated for 1 min at 90 °C, cooled down rapidly and applied onto 6% denaturing polyacrylamide gel (40-cm strips of gradient thickness of .15–.45 mm) (Grokhovsky et al., 1998). Electrophoresis was carried out for 60 min at 2500 V. Prior to exposure, the gel was fixed in 10% acetic acid and dried on a γ-methacrylpropyloxysilane-treated glass plate (LKB, Sweden).

Single-stranded oligonucleotides and double-stranded DNA constructs

The single-stranded oligonucleotides and double-stranded DNA constructs (S1 + S2) and (S5 + S2), (S5 + S9), (S4 + S9), (S3 + S6), (S10 + S11) и (S12 + S11), and (S3 + S7 + S8) were used as substrates in the studies of DNA binding and DNA unwinding catalyzed by UL9 helicase (Figure 3). The oligonucleotides S1–S12 were synthesized by the phosphoroamidite method and purified by electrophoresis in polyacrylamide gel (Syntol, Russia). The dyes were covalently attached to the 3′- and 5′-ends of the oligonucleotides S4 to S8 via aminohexamethylene linkers. Here, R6G and Cy5 are the derivatives of 6-carboxyrhodamine G and dye Cy5, respectively. Radioactively labeled oligonucleotides S1*, S2*, S3*, S7*, and S8* each containing a radioactive residue [γ-^{32}P]-AMP at the 5′-end. The analogs of R6G and Cy5 dyes were used as donors of electron excitation energy; the roles of the acceptors during the resonance energy transfer from the

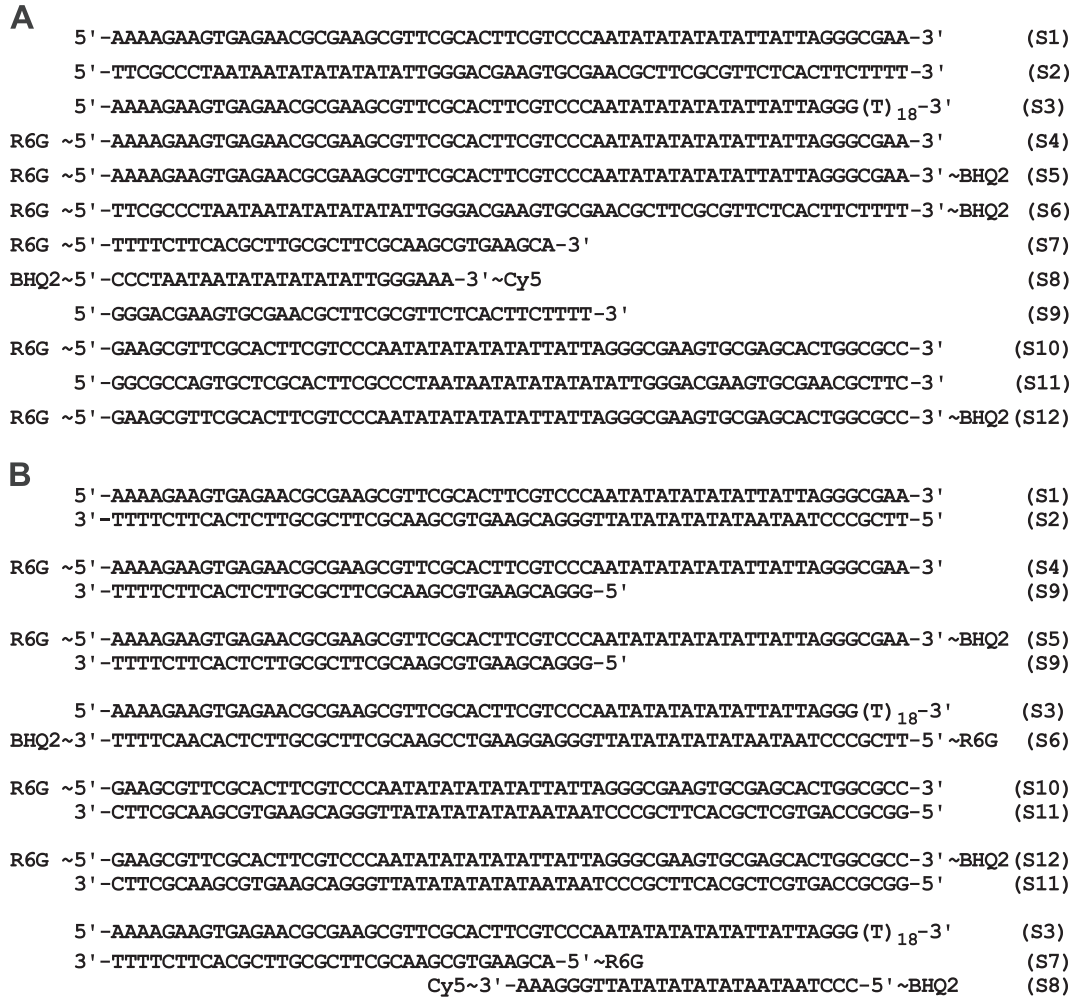

Figure 3. The single-stranded (A) and double-stranded oligonucleotide constructs (B) used as substrates in the studies of DNA binding and unwinding activities of the initiator protein UL9.

donor to the acceptor were played by the nonfluorescent dye BHQ2 (Black Hole Quencher 2) and Cy5 dye.

The efficiency of the energy transfer depends on the distance R between the donor and acceptor chromophores as $(R_0/R)^6$ (Förster, 1948), where R_0 is the critical distance between the donor and the acceptor wherein the probability of the nonradiative energy transfer from the donor to the acceptor is equal to the probability of spontaneous light emission by the excited donor in the absence of the acceptor. The numerical value of R_0 depends on the value of the overlap integral of the normalized fluorescence spectrum of the donor and the absorption spectrum of the acceptor, the quantum yield of the donor emission and the numerical coefficient K^2, which depends on the orientation of the transition moments of the donor emission and the acceptor absorption.

The gel electrophoretic mobility-shift assay (EMSA)

In order to prepare radioactively labeled oligonucleotides, 300 pmol of the oligonucleotide was mixed with 2 MBk (~15 pmol) of [γ-^{32}P]-ATP and 10 units of T4 polynucleotide kinase (Sibenzyme) in 20 mkl of phosphorylation buffer (50 mM Tris–HCl, pH 8.2, 10 mM $MgCl_2$, .1 mM EDTA, 5 mM DTT and .1 mM spermidine), the mixture was incubated at 37 °C for 1 h and then added 1 µl of 1 M unlabeled ATP solution and was incubated at 37 °C for 1 h.

Equimolar amounts of two or three single-stranded oligonucleotides (S3, S7 and S8) were mixed in 100 mM Tris-HCl buffer (pH 7.8). The oligonucleotides were annealed by heating at 90 °C and then allowing the samples to cool to room temperature overnight. The duplexes were isolated by nondenaturing 5% polyacrylamide gel with subsequent elution. Duplexes were precipitated with one volume of isopropanol, washed with 70% ethanol, dried, and dissolved in water. The duplexes were incubated with 2 µl OBP (3×10^{-6} M dimers) for 1 h at 39 °C in 50 mM Tris-HCl buffer (pH 7.8) in the presence of 5 mM dithiothreitol; 15 mM $MgCl_2$, 10% (v/v) glycerol; .01% (v/v) Triton X-100 and 10 mM ATP. The reaction mixtures (10 µl) were loaded in a nondenaturing 10% polyacrylamide gel with a .4 mm thickness. Radioactive bands were visualized by phosphoimager.

Helicase activity

The double-stranded oligonucleotide constructs (S1 + S2) and (S4 + S9), (S5 + S2), (S5 + S9), (S3 + S6) and oligomer (S3 + S7 + S8) were used as substrates in the studies of DNA binding and unwinding activities of OBP using the fluorescence methods, FRET and standard biochemical procedures based on the application of radiolabeled oligonucleotides and polyacrylamide gel mobility shift analysis of the reaction products (Belon, High, Lin, Pauwells, & Frick, 2010; Surovaya et al., 2010).

Experimental procedures

Absorption spectra were measured on a Jasco V-550 spectrophotometer. Fluorescence spectra were measured on a Cary Eclipse spectrofluorimeter. The experiments were performed in 20 mM Tris-HCl (pH 7.2), 4 mM $MgCl_2$, 10% glycerol, .18 M NaCl, .01% Triton X-100, and 1 mM dithiothreitol. Prior to the experiments, bis-netropsins were dissolved in a small volume of ethanol (≈20 µl) and then added in the buffer solution. The quenching of the donor fluorescence by the nonradiative transfer of the electron excitation energy from the donor to the acceptor (Förster, 1948) appeared to depend on the distance between the donor and the acceptor in the DNA oligomer alone and DNA–protein complex:

$$I_{DA}/I_D = 1/(1 + (R_0/R)^6) \tag{1}$$

Here, I_D is the fluorescence intensity of the donor in the absence of the acceptor, I_{DA} is the fluorescence intensity of the donor in the presence of the acceptor, R is the distance between the donor and the acceptor and R_0 is the critical distance between the donor and the acceptor wherein the probability of the resonance energy transfer from the donor to the acceptor is equal to the probability of spontaneous emission of the light by the donor in the absence of the acceptor.

$$R_0 = 9.79 \times 10^3 (K^2 n^{-4} q_D J)^{1/6} \ (\text{Å}) \tag{2}$$

$$J = \left(\int f(\lambda) \varepsilon_a(\lambda) \lambda^2 d\lambda \right) / \left(\int f(\lambda) d\lambda \right) \tag{3}$$

Here, q_D is the quantum yield of the donor fluorescence, n is the refraction index of the medium separating the donor and acceptor molecules, and K^2 is the numerical coefficient characterizing the mutual orientation of the transition moments of the donor emission and acceptor adsorption. For random mutual orientation of the transition moments, $K^2 = 2/3$. J is the overlap integral of the normalized fluorescence spectrum of the donor $f(\lambda)$ and the absorption spectrum of the acceptor $\varepsilon_a(\lambda)$ Where $\varepsilon_a(\lambda)$ is the molar extinction coefficient of the acceptor at wavelength λ. To estimate the efficiency of the energy transfer, $1 - I_{DA}/I_D$, the fluorescence intensities of the donor should be measured in two systems: one containing the oligonucleotide conjugated with a fluorophore and a quencher (I_{DA}) and another one containing the same oligonucleotide conjugated with the donor alone (I_D). Assuming random orientation of the transition moments of the donor and the acceptor, the distance between them can be calculated as:

$$R = R_0((I_{DA}/I_D)/(1 - I_{DA}/I_D))^{1/6} \tag{4}$$

where $(1 - I_{DA}/I_D)$ is the efficiency of the energy transfer between the donor and the acceptor; I_{DA} and I_D are the intensities of the donor fluorescence in the presence and absence of the acceptor, respectively, and R_0 is the critical distance between the excited molecule of the donor and the non-excited molecule of the acceptor wherein the probability of the energy transfer from the excited donor molecule to the nonexcited acceptor molecule is equal to the probability of spontaneous light emission from the excited donor molecule. The values of R_0 for the donor–acceptor pairs R6G–BHQ2 and R6G–Cy5 were found to be equal to 63 and 72 Å, respectively, provided that $n \approx 1.34$ and quantum yield of the donor fluorescence, $q_D \approx .8$. In the hairpin form of the oligonucleotide S8, chromophores Cy5 and BHQ2 are disposed at close proximity to one another. In this case, a contact-mediated quenching of fluorescence may occur instead of quenching caused by Förster mechanism of energy transfer (Marras, Kramer, & Tyagi, 2002).

Results and discussions

Specificity of binding of bis-netropsins to the viral origin of replication (OriS)

Figure 4 shows the footprinting diagrams of Pt-bis-Nt and Pt*-bis-Nt complexes with the DNA fragments containing an insert with the nucleotide sequence corresponding to the origin of replication OriS of HSV type 1. The DNA fragment used in our footprinting studies also contains oligonucleotide inserts carrying pseudosymmetrical sequences which may serve as potential interaction sites for Pt-bis-Nt and Pt*-bis-Nt.

As can be seen from Figure 4, both bis-netropsins protect the A + T cluster from cleavage by DNase I. From the concentration dependencies of the protective activity, we conclude that Pt-bis-netropsin at low extents of binding exhibits a stronger affinity for the A + T cluster and protects a longer DNA region than Pt*-bis-netropsin under the same conditions. Previous studies showed that Lys-bis-Nt and 15Lys-bis-Nt also bind selectively to long clusters of AT base pairs (Andronova et al., 2008; Surovaya, Grokhovsky, Bazhulina, & Gursky, 2008).

On the DNA fragment used in footprinting studies, Pt-bis-Nt protects the A + T cluster present in OriS as well as DNA segments containing two symmetry-related tetramers composed of adenine and thymine residues which are separated by one or two GC base pairs. One obvious example is the DNA segment carrying the sequence 5′-TATAGGTATA-3′. In this DNA region a clear footprint is observed at concentration as low as 3.3 μM Pt-bis-Nt. Interestingly, in the presence of Pt*-bis-Nt, the protective effect is not observed at this site, even at 3 times higher concentration.

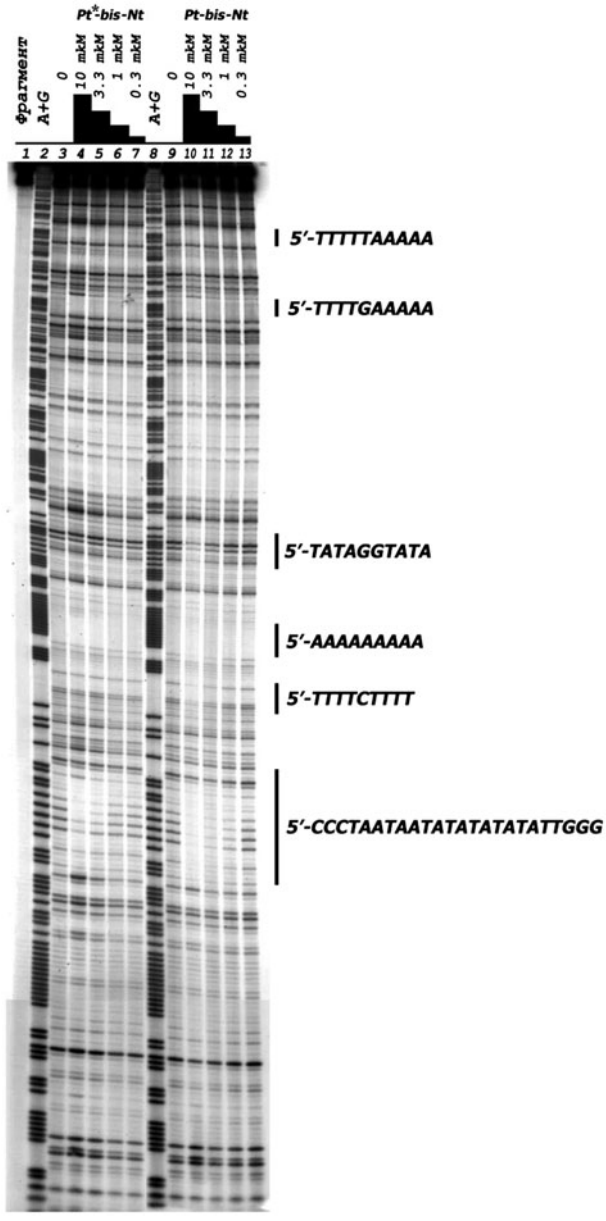

Figure 4. DNase I cleavage of the DNA segment containing the origin of replication OriS. Lane 1, untreated DNA fragment; lanes 2 and 8, A + G – purine sequence markers; lanes 3 and 9, cleavage products of the free DNA fragment; lanes 4–7, cleavage products in the presence of 10, 3.3, 1 and .3 μM Pt*-bis-Nt, respectively; lanes 10–13, cleavage products generated in the presence of 10, 3.3, 1 and .3 μM Pt-bis-Nt, respectively.

Helicase activity of the HSV1 UL9 protein

Annealing of the S5 and S2 oligonucleotides gives a duplex containing an A + T-rich segment and nucleotide sequences corresponding to Boxes I and III in OriS (Figures 1 and 3). In solution, the oligonucleotide S5 can spontaneously form hairpin-shaped structures one of which is enriched with GC pairs present in Boxes I and

III. Its melting temperature determined in this study is 83 °C. The second hairpin is enriched with AT base pairs, it is unstable and fully melts at 45 °C (Aslani et al., 2001, 2002). In free solutions, the oligonucleotides S5 and S6 assume stem and loop structures in which the 5′- and 3′-ends are held at a short distance from one another. This led us to suggest that under conditions where the binding of UL9 helicase to the duplex is coupled with strand separation and formation of a stem-loop structure in each strand, the donor and acceptor molecules tethered with the 5′- and 3′-ends of the oligonucleotide S5 become spatially approximated (Figure 1). This leads to the quenching of the donor fluorescence by the acceptor. The structure of the S5 oligonucleotide is reminiscent of a molecular beacon, viz., a hairpin-shaped single-stranded oligonucleotide labeled with a fluorophore at one end and a quencher at the other end. In solution, the oligonucleotide can form stem and loop structure stabilized by intramolecular pairing of Box I and Box III sequences. The stem holds the fluorophore and the quencher close to each other, a feature responsible for the quenching of the fluorophore fluorescence by the FRET mechanism. The loop portion of the beacon probe sequence can be designed to be complementary to the target single-stranded oligonucleotide. During hybridization, the loop portion of the beacon is paired with the target oligonucleotide segment. A rigid rod-like structure is formed between the beacon probe and the target oligonucleotide, while the beacon stem disrupted. As a consequence, the fluorescence intensity increases dramatically. This provides a basis for the application of molecular beacon probes as sensitive tools for detecting target sequences in single-stranded DNA. Molecular beacon probes can also be used to monitor helicase action (Belon et al., 2010). We found that the fluorescence intensity of the free S5 oligonucleotide is lower than that of the duplex (S5 + S9) carrying the fluorophore and the quencher which are separated by a larger distance. After addition of OBP to the S5 oligonucleotide and the (S5 + S9) duplex in the absence of ATP and ICP8, the fluorescence intensities decrease (Figure 5, panel A). Substantially lower quenching was observed on adding OBP to the oligonucleotide S4 and duplex (S4 + S9) containing no quencher. Evidently, in these systems, the quenching is not attributed to the energy transfer process and mediated by direct contact of OBP with the fluorophore. The fluorescence spectra of the (S5 + S9) duplex and the single-stranded oligonucleotide S5 recorded in the absence and presence of OBP are displayed in Figure 5, panel A. Curves 1 and 2 represent the fluorescence spectra of the (S5 + S9) duplex in the absence and presence of OBP; curves 3 and 4 correspond to the fluorescence spectra of the free oligonucleotide S5 0.18 M NaCl and its complex with OBP, respectively. Curves 5 and 7 represent the fluorescence spectra of (S4 + S9) duplex and oligonucleotide S4, respectively.

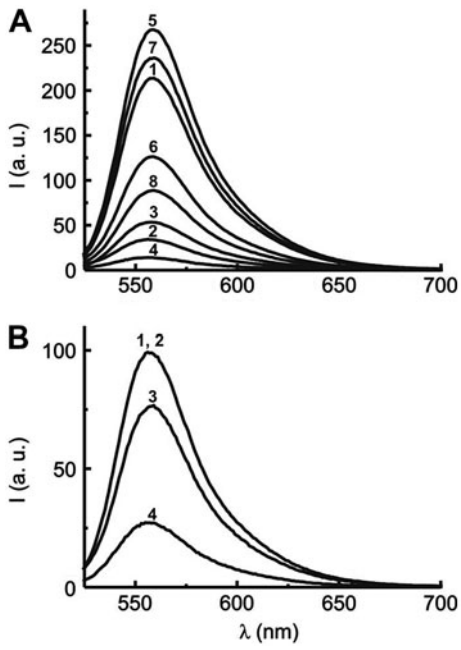

Figure 5. Panel A – the fluorescence spectra of the duplexes (S5 + S9) and (S4 + S9) (curves 1 and 5, respectively) and their complexes with OBP (curves 2 and 6, respectively). The fluorescence spectra of the free oligonucleotides S5 and S4 (curves 3 and 7, respectively) and their complexes with OBP (curves 4 and 8, respectively) are also shown. Panel B – the fluorescence spectra of the duplexes (S10 + S11) and (S12 + S11) (curves 1 and 2, respectively) and their complexes with OBP (curves 3 and 4, respectively). Excitation wavelength – 510 nm, excitation and emission slits are 10 and 5 nm, respectively, a. u. – arbitrary units. Concentrations: duplexes and free oligonucleotides – 2×10^{-7} M, OBP dimers – 4.9×10^{-7} M. Incubation conditions: 20 mM Tris-HCl (pH 7.2), 4 mM $MgCl_2$, 0.18 M NaCl, 10% glycerol, .01% Triton X-100, 1 mM dithiothreitol.

In the hairpin structure of the oligonucleotide S5 (or S6), the 5′- and 3′-ends are held close to each other. If the structure of the duplex is deformed upon binding of OBP dimers to DNA, the donor and acceptor molecules conjugated to the 5′- and 3′-ends of each oligonucleotide become spatially approximated (Figure 1), as can be evidenced from the quenching of the donor fluorescence by the acceptor. The fluorescence intensity of the free oligonucleotide S5 is substantially lower than that of the duplex conjugated with the same fluorophore and quencher which are separated by a larger distance from one another. The efficiency of the energy transfer from D to A in case of the free oligonucleotide S5 $(1 - I_{DA}/I_D)$ is equal to $.81 \pm .07$ suggesting that S5 exists in solution in the hairpin-like conformation. Similar results were obtained for the oligonucleotides S6 and S8. After addition of OBP to the single-stranded

oligonucleotide S5 and duplex (S5 + S9), the fluorescence intensity diminishes in the absence of ATP and ICP8 (Figure 5, panel A). It is noteworthy that the shape of the normalized fluorescence spectrum is not changed in the presence of the enzyme. The quenching may occur as a result of direct interaction of OBP with the fluorophore and/or may arise from a change in the DNA structure induced on binding of OBP, thus reflecting some change in the distance between the donor and acceptor chromophores. Our studies reveal that both mechanisms of quenching may occur. Their relative contribution to the overall amplitude of quenching can be determined experimentally.

In these studies, we also used duplexes formed upon annealing of the oligonucleotides S12 and S11 or S10 and S11 (Figure 5, panel B). These fluorescent DNA fragments contained Box I and Box II sequences which are separated by the A + T spacer. The weak binding site for helicase (Box III) was absent. The fluorescence spectra of the duplexes (S10 + S11) and (S12 + S11) recorded in the absence and presence of OBP are displayed in Figure 5. Here, curves 1 and 2 correspond to the fluorescence spectra of the duplexes (S10 + S11) and (S12 + S11) in the absence of helicase UL9. These spectra practically coincide. After addition of the OBP, the fluorescence intensity of the duplex (S12 + S11) carrying both the fluorophore and the quencher diminishes significantly (nearly 4-fold), while that of the system containing the (S10 + S11) duplex carrying no quencher, decreases by about 20% in the presence of OBP. Clearly, in the latter case, we deal with the quenching effect which is associated with the interaction of OBP with the fluorophore conjugated with (S10 + S11) duplex.

The distance between the donor and the acceptor can be measured by estimating the efficiency of the resonance energy transfer from the donor to the acceptor in the complex between helicase and duplex (S12 + S11):

$$R = R_0((I_{DA,OBP}/I_{D,OBP})/(1 - I_{DA,OBP}/I_{D,OBP}))^{1/6} \quad (5)$$

Here, $I_{D,OBP}$ and $I_{DA,OBP}$ are the fluorescence intensities of the donor in the complexes of OBP with the duplexes (S10 + S11) and (S12 + S11), respectively. The DNA oligomer concentrations and the molar ratio of helicase to DNA oligomer for these two complexes practically coincide. The estimated values of distances between the fluorophore and quencher are based on $R_0 = 63$ Å and $K^2 = 2/3$. This value of K^2 does not lead to a substantial error because the flurophore-quencher distance depends on inverse six power of K^2. The experimental value of $I_{DA,OBP}/I_{D,OBP}$ for complexes of OBP with the duplexes (S10 + S11) and (S12 + S11) is ≈.35 and the distance between the fluorophore and the quencher, $R \approx 57$ Å. Since linear DNA contains 63 base pairs, our FRET studies indicated that on binding of OBP dimers to Boxes I and II the DNA underwent structural changes for which interactions between bound helicase dimers are responsible. These results are supported by electron microscopy data suggesting that the interaction between OBP dimers bound to Boxes I and II results in DNA bending (by approx. 90°) and destabilization of AT base pairs in the AT spacer (Makhov, Boehmer, Lehman, & Griffith, 1996). In addition, there is evidence that binding of OBP to negatively supertwisted DNA-containing OriS converts the structure of the AT spacer into a form sensitive to digestion by micrococcal nuclease and to oxidation by potassium permanganate (Koff et al., 1991; Makhov et al., 1996).

Similar results were obtained for complexes of OBP with duplexes (S5 + S2) and partial duplex (S5 + S9) and (S4 + S9). In the absence of OBP, the distance between the fluorophore and the quencher in the partial duplex (S5 + S9) is equal to 79 Å. It markedly exceeds the value of 51 Å determined for the fluorophore-quencher distance in the single-stranded oligonucleotide S5. In the presence of OBP (4.9×10^{-7} M), the fluorescence intensity measured for partial duplex (S5 + S9) decreases reflecting the change in a distance between the fluorophore and quencher. The experimental value of $I_{DA,OBP}/I_{D,OBP}$ is .26, and the distance between the fluorophore and the quencher, R, is equal to approximately 53 Å. This is close to the value obtained for hairpin-like form of the oligonucleotide S5. After incubation of the reaction mixture containing (S5 + S9) duplex, OBP and ATP for 240 min the experimental value of $I_{DA,OBP}/I_{D,OBP} \approx .69$ and the fluorophore-quencher distance in the complex of OBP with the (S5 + S9) duplex takes up a value ≈72 Å.

A model consistent with the FRET data is that in which two DNA duplexes each forming the 1:1 complex with OBP dimer associate to form a 4-ways Holiday junction (HJ) containing Box I and Box III inverted repeats. It is noteworthy that OriL contains two pairs of Box I and Box III sites which are separated by AT-rich segment. In contrast, OriS contains Box I and Box II sequences separated by AT-rich segment, but it has only a single copy of Box III sequence. X-ray diffraction studies show that two DNA strands in the antiparallel 4-ways HJ preserve their usual helical conformations, with the other two strands undergoing conformation changes and serving as the crossover strands (Ortiz-Lombardia et al., 1999). Based on the results of FRET experiments, we suggest that HSV1 OBP and its homologs in other alpha- and betaherpes viruses belong to a family of DNA HJ-binding proteins. Examples of proteins of this family class are the *E. coli* helicases RuvAB, UvrD, and RecG which play key roles in DNA recombination, repair and replication processes (Carter, Tahmaseb, Compton, & Matson, 2012; Mahdi, McGlynn, Levett, &

Lloyd, 1997; Rafferty et al., 1996; Whitby & Lloyd, 1998). In addition, it should be noted that DNA recombinase Cre (Gopal, Guo, & Van Duyne, 1998) and some endonucleases bind and resolve HJs (Bennett & West, 1995; Biertümpfel, Yang, & Suck, 2007; Hadden, Déclais, Carr, Lilley, & Phillips, 2007). The *E. coli* protein RuvA recognizes HJ and in combination with another protein RuvB catalyzes migration of branch point and unwinding of HJ (Nishino, Ariyoshi, Iwasaki, Shinagawa, & Morikawa, 1998; Rafferty et al., 1996). In the 3D structure of a complex formed by RuvA tetramer with synthetic HJ, the alpha-helix-hairpin-alpha-helix (HhH) domains of RuvA monomers are implicated in hydrogen bonding and electrostatic interaction with sugar-phosphate backbone of four HJ arms (Ariyoshi, Nishino, Iwasaki, Shinagawa, & Morikawa, 2000; Nishino et al., 1998; Rafferty et al., 1996). Each RuvA monomer contains two consecutive HhH domains related by approximate twofold symmetry which are bridged by a connector alpha helix (Ariyoshi et al., 2000; Doherty, Serpell, & Ponting, 1996; Rafferty et al., 1996; Shao & Grishin, 2000). This structural unit is designated as the $(HhH)_2$ motif. A characteristic feature of $(HhH)_2$ motif is that the hairpin loops are enriched by glycine and proline residues and often contain hydrophobic residues surrounded by two glycine residues (Doherty et al., 1996; Shao & Grishin, 2000). In the $(HhH)_2$ motif of RuvA monomer, the hairpin loops are separated by 30 residues. The structure of $(HhH)_2$ motif is known to be stabilized by interactions between hydrophobic residues present in characteristic positions in alpha helices and hairpin loops (Nishino et al., 1998; Rafferty et al., 1996; Shao & Grishin, 2000). An important property of HJ is its ability to undergo branch migration through regions of sequence homology. This process involves the melting and annealing of base pairs and results in movement of the branch point along the arms of the junction. The HJ may be considered as an intermediate for conversion of each DNA strand into the hairpin-like form stabilized by complementary pairing of Box I and Box III sequences in OriS.

Figure 6 shows that HSV1 OBP and its homologs in other herpes viruses exhibit sequence similarities with DNA HJ-binding proteins RuvA, UvrD, and RecG of *E. coli* and *Helicobacter pylori*.

The similarities between the sequences implicated in the $(HhH)_2$ motif of the HJ-binding protein RuvA and DNA-binding domains of the viral replication origin binding proteins suggest that HSV1 OBP and its homologs in other viruses belong to a family of the HJ-binding helicases. Interesting that peptide RVKNLTK flanking the second hairpin in the presumed $(HhH)_2$ motif of HSV1 OBP is known to be implicated in the recognition of the viral DNA replication origin (Olsson et al., 2009). Our recent experiments show that HSV1 OBP binds more strongly to a synthetic HJ than to a linear DNA and catalyzes the unwinding of HJ in the presence of ATP (Moiseeva et al., 2013).

EMSA analysis of complexes formed by HSV1 OBP with single-stranded oligonucleotides S1 and S2 and duplex (S1 + S2)

The fluorescence spectra measured for the single-stranded oligonucleotide S5 and its complex with UL9 helicase are indicative of substantial quenching. The eletrophoretic mobilities of single-stranded oligonucleotides $S1^*$ and $S2^*$ and their mixtures with OBP are distinctly different (Figure 7). We have found that OBP forms a strong complex with the single-stranded oligonucleotide S1 and exhibits a lower affinity for binding to the (S1 + S2) duplex. The values of the corresponding association constants differ nearly 10-fold as revealed from competition-type experiments, using ethidium bromide as a competitive ligand (Surovaya et al., 2010). Such a difference in the affinities of OBP to the (S1 + S2) duplex and single-stranded oligonucleotides S1 seems to be the main cause of structural changes induced on binding of OBP to the (S1 + S2) duplex. These structural changes involve DNA bending and formation of 3D structure containing both single-stranded and base paired DNA segments.

Analysis of the melting curves for (S1 + S2) duplex showed that on average three base pairs in the (S1 + S2) duplex exist in an unwound state at 42°C and may serve as a "nucleus" for helix-coil transition within the A + T cluster in (S1 + S2) duplex. Incubation of the ($S1^* + S2^*$) duplex with OBP and ATP (60 min, 42 °C) gives a small quantity of the product whose mobility during polyacrylamide gel electrophoresis coincides with the mobility of a complex between OBP and single-stranded oligonucleotide S1 (Figure 7).

In the oligomer (S3 + S7 + S8) and partial duplexes (S5 + S9), (S4 + S9), and (S3 + S6) the upper oligonucleotide strand contains single-stranded tail at 3′-end. To obtain the (S3 + S7 + S8) oligomer or (S5 + S9) duplex, the complementary strands at equimolar concentrations were annealed at 90°C with subsequent 8–10 h cooling to room temperature.

Unwinding of the AT-rich hairpin by OBP in the absence and presence of Pt-bis-netropsin

The time curses of the S5 fluorescence intensity at 559 nm after addition of OBP and ATP in the absence and presence of Pt-bis-Nt are displayed in Figure 8.

The experimentally determined dependencies of the fluorescence intensity on time can be described by the equation:

$$I_{559}(t) = A_0 + A_1 \exp(-t/T_1) \qquad (6)$$

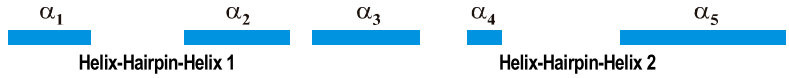

71	LFKELIKTN	GVGP	KLALAILSGMSAQQFVNAVEREEVGALVKL	PGIG	KKTAERLIVEMKDRFK	133	E.coli RuvA
709	VADALSGCP	PRGS	VSETDHAVALFKIIWGELFGVQMAKSTQTF	PGAG	RVKNLTKQTIVGLLDA	771	HSV1 OBP
705	ALSALGAGG	GAGP	LSRGRHAALVFKVMWEEAFGVRVGRSRQTF	PGPT	RVKNLRKAEIAALLRD	767	SHV1 OBP
692	FLDGCHNQC	FRPI	PTKHEYNIALFRLIWEQLFGARVTKSTQTF	PGST	RVKNLKKKDLETLLDS	754	VZV OBP
713	LSGRGFAQG	RGVG	LGAAAHAVSVFKVIWEEVFGARLQKSTQTF	PGHA	RVKNLRKHEIVALLDL	775	BHV1 OBP
744	TTALSGRPK	SRVP	LSKGEHAVSLFKVLWEDVFGAKLAKSTQTF	PGGV	RVKNLRKDEIVALLES	806	EHV1 OBP
658	FNKLRGMRI	VTGV	FSIEKFSISILRLPPKCAFNMTLSASKPRY	IPGK	AYRNLTKNDLENMLDN	720	HHV6 OBP
660	NRLKGMQLN	TWSL	SIAKFSVSIIRMFFKCAFNMNLVKSKPRYI	VGKP	FRSLTKREIETLLDMW	722	HHV7 OBP
417	ERVVNTPTR	GIGD	RTLDVVRQTSRDRQLTLWQACRELLQEKAL	AGRA	ASALQRFMELIDALAQ	479	E.coli UvrD
409	ALWEKGQQQ	GFHP	HQLIMTATPIPRTLAMTAYADLDTSVIDEL	PPGR	TPVTTVAIPDTRRTDI	471	E.coli RecG
364	QLEKMASSK	GNKP	HSLQFSATPIPRTLALAKSAFVKTTMIREI	PYPK	EIETLVLHKRDFKIVM	426	H.pylori RecG
69	LFERLLKIN	GVGG	RIALAILSSFSPNEFENIIATKEVKRLQQV	PGIG	KKLADKIMVDLIGFFI	131	H.pylori RuvA

Figure 6. Sequence similarities of the DNA HJ-binding helicases RuvA, UvrD, and RecG of *E. coli* and *Helicobacter pylori* with the HSV1 replication origin binding protein, OBP, and its homologs in some alpha- and beta-herpes viruses. The abbreviations and accession numbers used are: HSV1, herpes simplex virus type 1, human herpesvirus 1, NC_001806; BHV1, bovine herpesvirus 1, NC_001847; EHV1, Equid herpesvirus 1, NC_001491; VZV, varicella zoster virus, human herpesvirus 3, NC_001348; SHV1, Suid herpesvirus 1, pseudorabies virus, NC_006151; HHV6A, human herpesvirus 6A, NC_001664; HHV6B, human herpesvirus 6B, NC_000898; HHV7, human herpesvirus 7, NC_001716. Replication origin binding proteins of viruses HHV6A and HHV6B have identical sequences. Indicated are the helical regions α_1, α_2, α_3, α_4 and α_5 and the hairpin loops in the RuvA $(HhH)_2$ motif, as revieled from crystallographic studies of a complex between a single RuvA tetramer and HJ (Ariyoshi et al., 2000).

where $I_{559}(t)$ is the fluorescence intensity of the oligonucleotide complexes with helicase in the absence and presence of Pt-bis-Nt, t is the time from the moment of ATP addition to the solution under study, T_1 is the characteristic time of the process, A_0 is the limiting value of $I_{559}(t)$ when t approaches infinity, A_1 is the constant. The solid curves in Figure 8 represent theoretically calculated dependencies $I_{559}(t)$ wherein the sum of the squares of the deviations of the experimental points from the calculated values $I_{559}(t)$ approaches the minimum.

The values of A_0, A_1 and T_1 corresponding to the best fit curves are indicated in Figure 8.

The shape of the experimental curves suggests that Pt-bis-netropsin decreases the rate of ATP-dependent unwinding of the AT-rich hairpin by OBP. The mean value of T_1 is 169.6 ± 22.7 min (data from three independent experiments), while T_1 measured in the absence of Pt-bis-Nt is 113.5 ± 14.7 min. The difference between the mean values of T_1 can be considered as a quantitative measure of the decrease in the rate of the unwinding reaction caused by Pt-bis-Nt binding to the AT-rich hairpin. Previous studies established that upon binding to the AT-rich hairpin Pt-bis-Nt increases its stability, as can be evidenced from the rise of the melting temperature by nearly 20 °C (Surovaya et al., 2008). 15Lys-bis-Nt and Lys-bis-Nt have a similar effect (Surovaya et al., 2010). Consistent with this are our observations that T_1 value for ATP-dependent DNA unwinding process is increased on lowering the temperature of the reaction mixture from 37° to 33 °C (Figure 8, panel C). This can be attributed to a higher extent of the stability of AT-rich hairpin at 33 °C.

Structural changes induced in the DNA upon binding of OBP in the absence and presence of ATP and Pt-bis-netropsin

The time courses of the fluorescence intensities of the reaction mixtures containing single-stranded oligonucleotide S6 and duplex (S3 + S6) in the presence of OBP and ATP are shown in Figure 9 (panels A and B). In the absence of OBP, substantial quenching is observed in the single-stranded oligonucleotide S6 in comparison with duplex (S3 + S6). It reflects the fact that oligonucleotide S6 exists in a hairpin-like conformation in solution. Addition of OBP to the (S3 + S6) duplex leads to approximately fivefold decrease in the intensity of fluorescence at 559 nm, whereas a ninefold decrease in the fluorescence intensity is observed for a mixture of the single-stranded oligonucleotide S6 and OBP under the same conditions.

As can be seen from Figure 9, the fluorescence intensity of a complex between (S3 + S6) duplex and OBP measured immediately after addition of ATP increases and then a slow time-dependent quenching of the fluorescence is observed. After 300-min incubation, the distance between the donor and the acceptor becomes closer to the value observed for the free oligonucleotide S6. The slope of the straight line $I_{559}(t)$ in the system containing Pt-bis-Nt takes up a ~1.5 time lower value in comparison with the system containing no Pt-bis-netropsin. This reflects the fact that upon binding to the (S3 + S6) duplex Pt-bis-netropsin stabilizes structure of A + T-rich DNA segment and diminishes the rate of DNA unwinding by OBP.

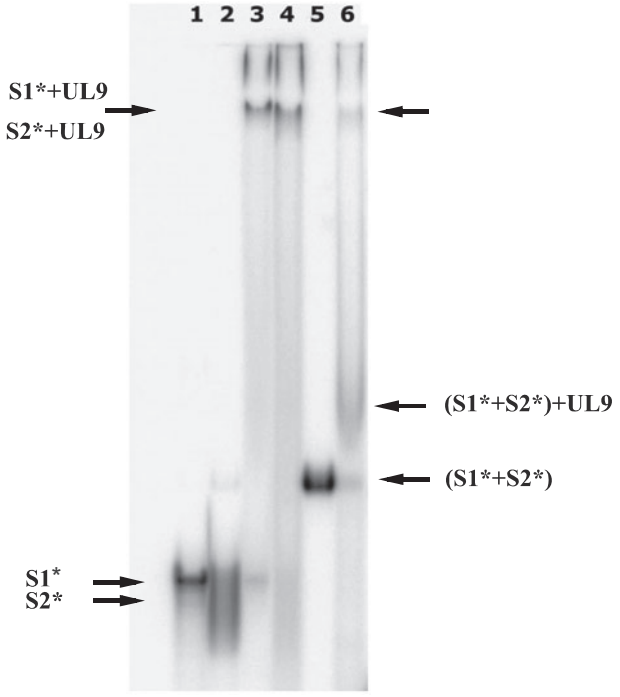

Figure 7. Electrophoresis analysis in nondenaturing 10% polyacrylamide gel of single-stranded oligonucleotides S1* and S2*, duplex (S1* + S2*) and their complexes with helicase UL9. Lanes 1 and 2, electrophoresis mobilities of the free oligonucleotides S1* and S2*, respectively. Lanes 3 and 4, mobilities of complexes of the oligonucleotides S1* and S2* with the protein UL9, respectively. Lanes 5 and 6, mobilities of the duplex (S1* + S2*) in the absence and presence of OBP, respectively. The mixture of OBP with duplex (S1* + S2*) was incubated for 60 min at 42 °C in 50 mM Tris-HCl buffer (pH 7.8) in the presence of 5 mM dithiothreitol; 15 mM $MgCl_2$, 10% (v/v) glycerol; .01% (v/v) Triton X-100 and 3 mM ATP. The reaction mixture was then cooled to 25° C and loaded on a 10% nondenaturing polyacrylamide gel with a .4 mm thickness and acryl/bis-acrylamide ratio of 29:1. Electrophoresis was carried out for 130 min at 650 V and temperature 22 °C.

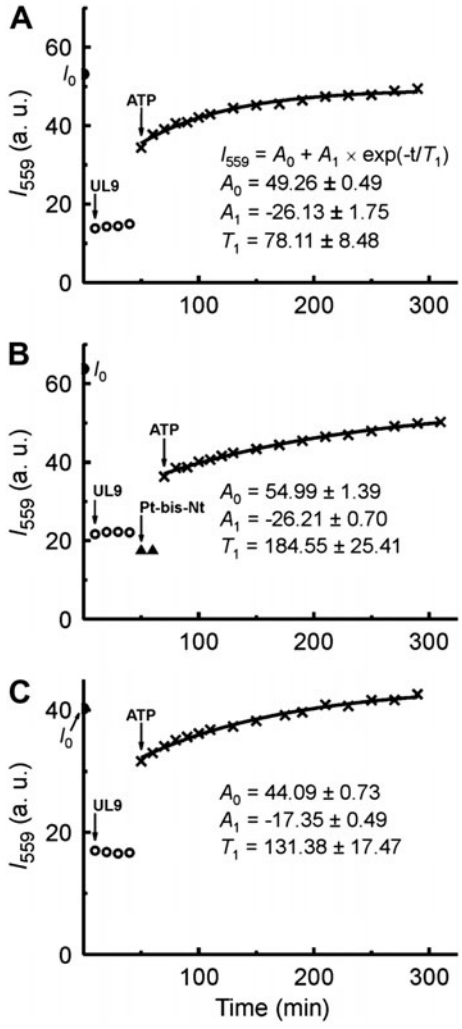

Figure 8. The kinetics of unwinding of the AT-rich hairpin in the S5 oligonucleotide by helicase UL9 in the absence (A) and presence (B) of Pt-bis-netropsin. I_0 – fluorescence intensity of free S5 at 559 nm. Excitation wavelength – 510 nm; excitation and emission slit widths – 10 and 5 nm, respectively. Additions of OBP, Pt-bis-Nt and ATP to the oligonucleotide solution are indicated by arrows. Concentrations: ATP – 1.8×10^{-2} M, S5 – 1.1×10^{-7} M, UL9 helicase – 3.9×10^{-7} M, Pt-bis-Nt – 2.9×10^{-7} M. Incubation conditions: 20 mM Tris-HCl (pH 7.2), 4 mM $MgCl_2$, .18 M NaCl, 10% glycerol, .01% Triton X-100, 1 mM dithiothreitol, 37 °C. Panel C, the kinetics of unwinding of the AT-rich hairpin in the oligonucleotide S5 measured at 33 °C in the absence of Pt-bis-Nt.

Consistent with these results are the observations obtained for the (S3 + S7 + S8) oligomer which differs from the (S3 + S6) duplex in that the oligonucleotides S7 and S8 replace oligonucleotide S6 in a complex with the oligonucleotide S3 (Figure 10). After annealing of the oligonucleotides S3, S7, and S8, the upper strand of the oligomer contained a 3′-terminal single-stranded tail of 18 nucleotides long. The analogue of the cyanine dye Cy5 is tethered to the 3′-end of the oligonucleotide S8, whereas the donor (R6G) is attached to the 5′-end of the oligonucleotide S7. The observed quenching effect reflects a change in the efficiency of energy transfer from the excited donor to the acceptor attached to the 5′- and 3′- ends of the oligonucleotides S7 and S8. Consistent with this are the observations that a decrease of the fluorescence intensity at 559 nm is accompanied by an increase of the fluorescence intensity at 670 nm (Figure 10, panels A and C). This can be attributed to the energy transfer from the excited donor (R6G) to the acceptor (Cy5) conjugated with oligonucleotides S7 and S8, respectively.

Two time-dependent processes were observed: the quenching of the fluorescence at 559 nm that can be associated with the formation of HJ by two oligomers (S3 + S7 + S8) complexed with OBP and the unwinding of the HJ by OBP in the presence of ATP.

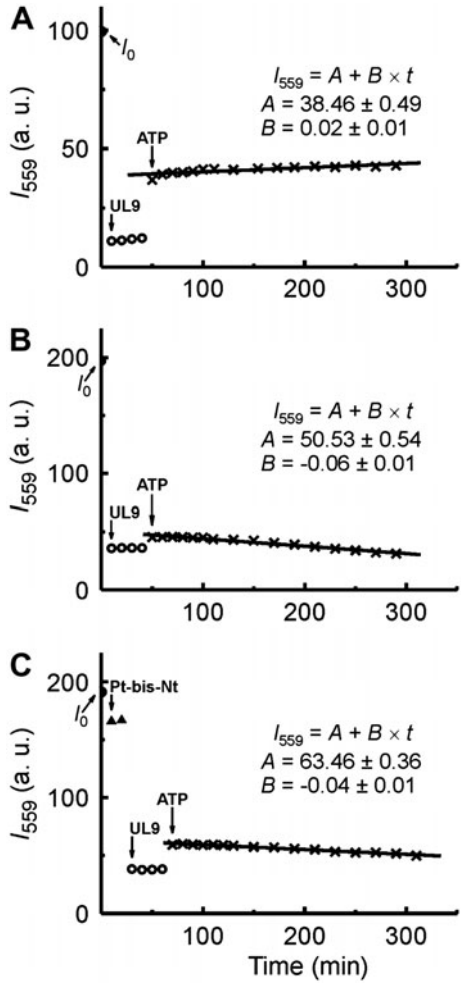

Figure 9. The time courses of fluorescence intensities of free oligonucleotide S6 (panel A) and double-stranded construct (S3 + S6) reflecting the ATP-dependent unwinding of double-helical DNA by OBP in the absence (panels A and B) and in the presence of Pt-bis-netropsin (panel C). I_0 designate the intensity of the fluorescence of the free oligonucleotide S6 and (S3 + S6) duplex at 559 nm. Excitation wavelength – 510 nm, excitation and emission slit widths – 10 and 5 nm, respectively. Concentrations: ATP – 1.8×10^{-2} M, S6 oligonucleotide and (S3 + S6) duplex – 1.1×10^{-7} M, OBP (dimers) – 3.9×10^{-7} M, Pt-bis-Nt – 8.9×10^{-7} M. The solid lines (panels A, B, and C) represent the best fit curves $I_{559}(t)$ for which the sum of squares of the deviations of the calculated values of $I_{559}(t)$ from experimental data points approaches the minimum. Experimental conditions are indicated in the legend to Figure 8.

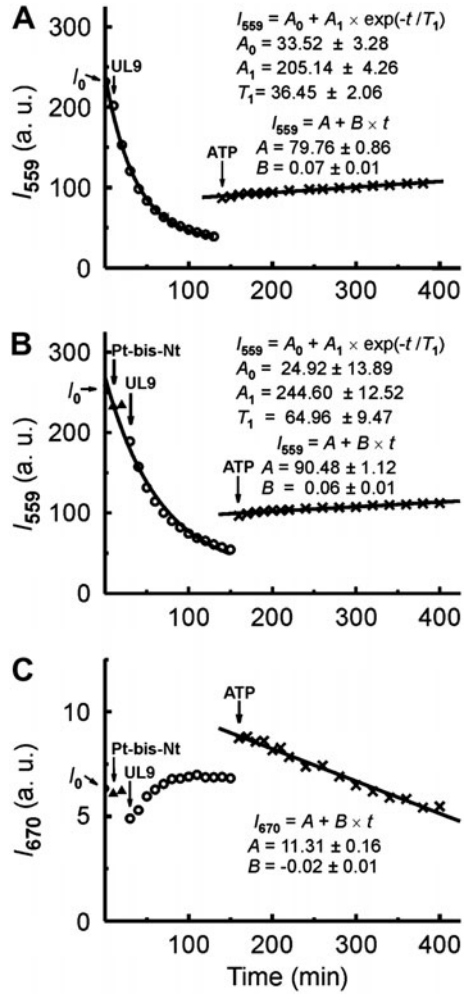

Figure 10. Changes in the (S3 + S7 + S8) oligomer structure and aggregation state which are induced by OBP in the absence (A) and presence of Pt-bis-netropsin (B) and ATP. I_0 is the fluorescence intensity of the free (S3 + S7 + S8) oligomer at 559 nm. Excitation wavelength – 510 nm, emission and excitation slit widths are 5 and 10 nm, respectively. Additions of OBP, Pt-bis-Nt and ATP to the (S3 + S7 + S8) oligomer solutions are indicated by arrows. Concentrations: ATP – 1.8×10^{-2} M, (S3 + S7 + S8) – 1.1×10^{-7} M, UL9 helicase – 3.95×10^{-7} M, Pt-bis-Nt – 8.9×10^{-7} M. The solid lines corresponding to the dependencies on time $I_{559}(t)$ (panels: A and B) and $I_{670}(t)$ (panel C) show the best fits to the experimental data points. Conditions are indicated in the legend to Figure 8.

In the presence of Pt-bis-netropsin, the quenching process induced after addition of OBP proceeds more slowly. The characteristic time of the reaction (T_1) increases from 36 to 65 min (Figures 10, panels A and B). The addition of ATP to the reaction mixture containing OBP and (S3 + S7 + S8) oligomers leads to an increase of the fluorescence intensity at 559 nm, reflecting a change in the distance between the fluorophore and quencher. The average distance between the donor (R6G) and the acceptor (Cy5) may increase due to a partial dissociation of the oligonucleotide S8 from the ternary complex (S3 + S7 + S8).

Figure 11 shows the EMSA analysis of the products present in the reaction mixture after incubation of the oligomer ($S3^* + S7^* + S8^*$) with OBP and ATP for 30 min at 37 °C and subsequent cooling of the reaction mixture to room temperature. EMSA studies show that the amount of free radioactively labeled oligomers ($S3^* + S7 + S8^*$) in the solution decreased after addition

of OBP. Slowly migrating species are formed that may represent a 4-ways HJ built by two oligomers ($S3^* + S7^* + S8^*$) each forming a 1:1 complex with OBP. After incubation of the reaction mixture at 37 °C for 30 min in the presence of ATP and Mg^{+2} ions, the presumed complex of HJ with OBP (designated as X+UL9) partially dissociates, and a slowly migrating complex of OBP with a folded form of oligonucleotide $S3^*$ is observed. In addition, free ($S3^* + S7^* + S8^*$) oligomers and oligonucleotide $S8^*$ are also present in the reaction mixture (Figure 11, panel C). The dissociation of HJ in the presence of ATP and Mg^{+2} ions is reminiscent of complexes of UvrD and RecG helicases with synthetic HJs (Carter et al., 2012; Whitby & Lloyd, 1998).

In the presence of Pt-bis-Nt, the intensities of bands corresponding to the free oligonucleotide $S8^*$ and complex of OBP with the oligonucleotide $S3^*$ are diminished, whereas intensity of the band corresponding to the free oligomer ($S3^* + S7^* + S8^*$) and its complex with Pt-bis-Nt is increased (data are not shown).

Measurements of the fluorescence intensity at 670 nm, $I_{670}(t)$, after addition of ATP-enabled monitoring the kinetics of the ATP-dependent DNA unwinding by OBP using fluorescent DNA substrates. The kinetic curves for the ATP-dependent unwinding of the (S3 + S7 + S8) oligomer in the absence and presence of Pt-bis-netropsin are shown in Figure 12 (panels A and C).

Here, I_0 is the fluorescence intensity of the free (S3 + S7 + S8) oligomer excited at 620 nm and measured at 670 nm. ATP added to the reaction mixture in the absence of Pt-bis-netropsin stimulated the time-dependent quenching of the fluorescence at 670 nm, which

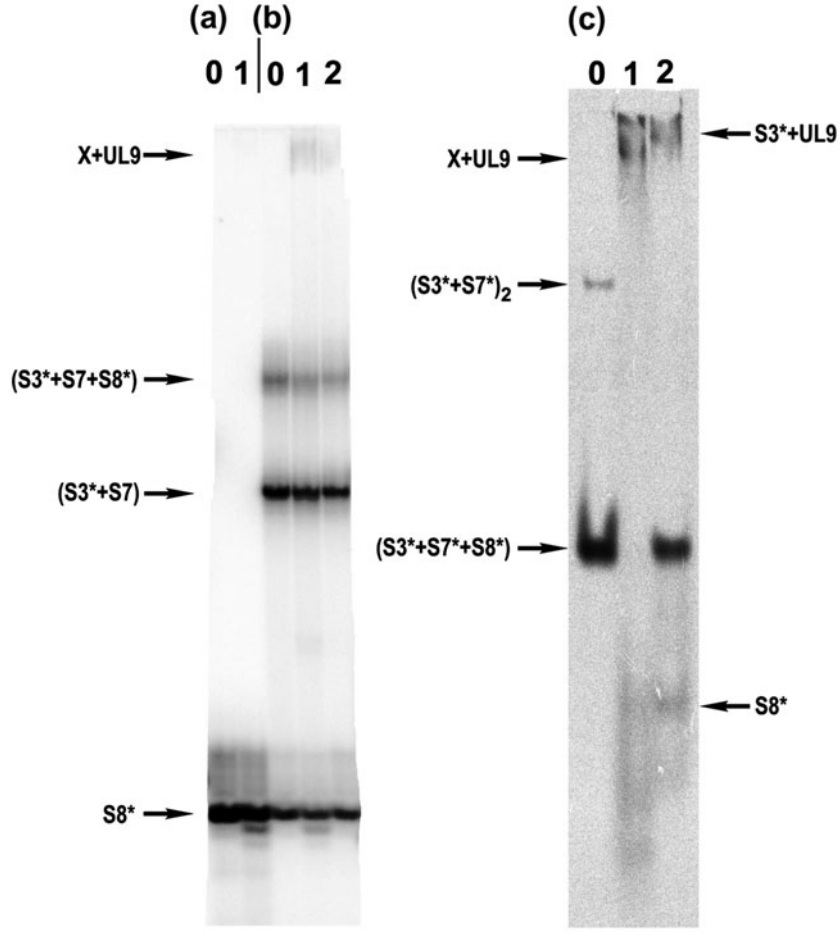

Figure 11. EMSA studies in the nondenaturing 10% polyacrylamide gel of complexes formed by OBP with single-stranded oligonucleotide S8 (panel a), partial duplex ($S3^* + S7$) and oligomer ($S3^* + S7 + S8^*$) (panel b). Lane 0, oligonucleotide $S8^*$ alone (panel a), ternary complex ($S3^* + S7^* + S8^*$) and partial duplex ($S3^* + S7$) in the absence of OBP and ATP (panel b). In panels a, b, and c, lane 1 corresponds to a complex of OBP with single-stranded oligonucleotide $S8^*$ (panel a), duplex ($S3^* + S7^*$) (panel b) and oligomer ($S3^* + S7^* + S8^*$) (panel c) in the absence of ATP. Lane 2 corresponds to the same complex incubated for 30 min at 37 °C in 50 mM Tris-HCl buffer (pH 7.8) in the presence of 5 mM dithiothreitol, 15 mM $MgCl_2$, 10% (v/v) glycerol; .01% (v/v) Triton X-100 and 20 mM ATP. The reaction mixtures were cooled to room temperature and loaded on a 10% nondenaturing polyacrylamide gel (19:1) with a thickness of .4 mm. Electrophoresis was carried out for 120 min at 800 V and temperature 20 °C.

reflected the unwinding and partial dissociation of the S8 oligonucleotide. In the free solution, the S8 oligonucleotide can spontaneously fold into a hairpin-like structure. The conversion is accompanied by quenching of the Cy5 fluorescence (Figure 12, panel A). Reannealing of the oligonucleotides S3, S7, and S8 to form a ternary complex was eliminated due to the presence of stem and loop structures in these oligonucleotides in solutions.

At bis-netropsin/DNA oligomer molar ratio equal to 1.2 the ATP-dependent unwinding of the oligomer (S3 + S7 + S8) by OBP appeared to be inhibited virtually completely (Figure 12, panel C). It is noteworthy that Pt-bis-Nt also decreased the rate of unwinding of the AT-rich hairpin in the oligonucleotide S5 (Figure 8) and prevented formation of an extended non-structured tail at the 3′-end of the oligonucleotide.

Antiviral activity of bis-netropsins

Footprinting studies have revealed that Pt-bis-netropsin binds selectively to the A + T cluster in OriS and inhibits the fluctuation opening of the AT pairs which is a prerequisite to DNA unwinding by OBP. In the presence of Pt*-bis-Nt, less apparent protective effects are seen in comparison with Pt-bis-netropsin. The binding constant of Pt-bis-netropsin is $\approx 10^8\,M^{-1}$, that is, $\sim$10 times higher than that found for Pt*-bis-Nt. It is noteworthy that 15Lys-bis-Nt, Pt-bis-Nt and Lys-bis-Nt also possess antiherpetic activity in cultured Vero E6 cells ($IC_{50} = 1.3$, 4.4 and 11.6 μM, respectively); the values of the selectivity indexes (SI) for 15Lys-bis-Nt, Pt-bis-Nt and Lys-bis-Nt are equal to 47, 59 and 29, respectively. Pt*-bis-Nt exhibits low (if any) antiviral activity against HSV1-infected Vero E6 cells ($SI \approx 0$) (Andronova et al., 2008; Surovaya et al., 2010). We also studied the cell toxicity of 15Lys-bis-Nt and Lys-bis-Nt in the cultured Vero E6 cells. Cell viability estimated by trypan blue exclusion method was significantly lowered in the presence of Nt, as compared with 15Lys-bis-Nt and Lys-bis-Nt. The values of cytotoxic concentration CC_{50} (the concentration sufficient to induce death of 50% of cells after 72 h incubation) for 15 Lys-bis-Nt and Lys-bis-Nt are equal to 176 and 362 μg/ml, respectively, being in case of administration of Lys-bis-Nt approximately by one order of magnitude higher than that found for Nt (37.5 μg/ml). *In vitro* studies of antiviral activities of dimeric netropsin derivatives against the HSV1 strain L_2 established that after infection of cultured Vero E6 cells with multiplicity of infection of about .1 PFU/cell, both 15Lys-bis-Nt and Lys-bis-Nt provided selective inhibition of virus replication. The concentrations of the bis-linked netropsin derivatives sufficient to suppress the virus-induced cytopathic effect by 50% in comparison with control, CI_{50}, were commensurate to the value obtained for the parent antibiotic Nt (3.7, 12.5 and 5.0 μg/ml for 15Lys-bis-Nt, Lys-bis-Nt and Nt, respectively). However, the selectivity index calculated as the CC_{50}/CI_{50} ratio was significantly lower for netropsin as compared with the corresponding values for 15Lys-bis-Nt and Lys-bis-Nt (7.5 against 47 and 29, respectively). It is noteworthy that a similar selective antiviral effect was observed for HSV1 strains resistant to basic antiherpetic drugs (acyclovir, phosphonoformic acid, etc.).

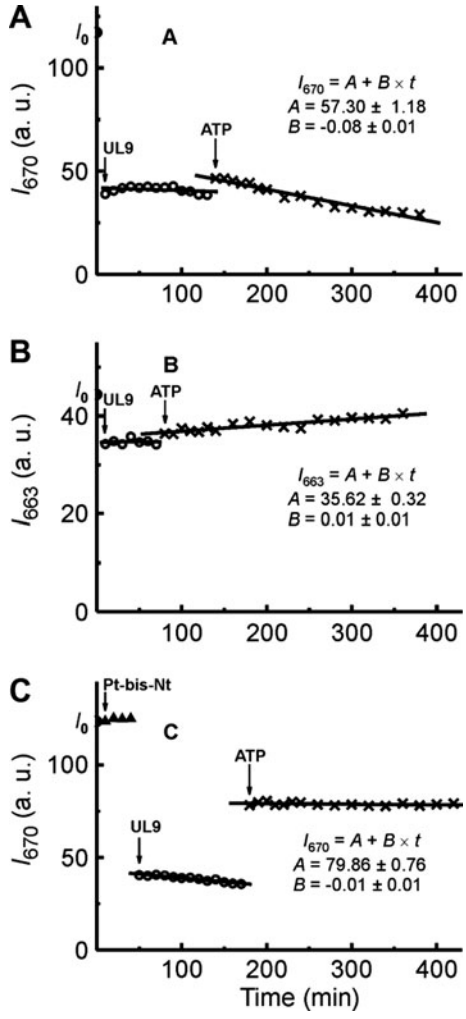

Figure 12. The unwinding of DNA in the (S3 + S7 + S8) oligomer in the absence (A) and presence of Pt-bis-netropsin (C) I_0 – intensity of fluorescence of the free (S3 + S7 + S8) oligomer at 670 nm. Excitation wavelength – 620 nm, excitation and emission slit widths – 10 and 5 nm, respectively. Panel B – time course of the fluorescence intensity of the free oligonucleotide S8 at 663 nm in the presence of helicase and ATP. The solid lines show the calculated curves $I_{670}(t)$ (panels A and C) and $I_{663}(t)$ (panel B) providing the best fit to the experimental data. Concentrations of components of the reaction mixture in the absence of Pt-bis-netropsin are as follows: ATP – 1.8×10^{-2}, (S3 + S7 + S8) and S8 – 1.1×10^{-7}, OBP – 3.97×10^{-7} M. In the presence of Pt-bis-netropsin concentrations are as follows: ATP – 1.9×10^{-2} M, (S3 + S7 + S8) – 1.15×10^{-7} M, OBP – 3.44×10^{-7} M, Pt-bis-Nt – 1.4×10^{-7} M. Conditions are indicated in the legend to Figures 8.

As regards the therapeutic effect of 15 Lys-bis-Nt and Lys-bis-Nt on HSV1-infected BALB/c mice, 15Lys-bis-Nt (30 mg/kg wt) injected intraperitoneally two times a day for 5 days (the first dose was administered 2 h after the infection) reduced mortality by 45% (cf. 60% in the control group (infected but untreated mice) (Andronova et al., 2012; Andronova, Grokhovsky, Surovaya, Gursky, & Galegov, 2013).

In this study, 15Lys-bis-Nt and Lys-bis-Nt were used in the form of .075% and .15% polyethyleneglycol (PEG-600)-based ointments. Their pronounced curative effect on skin injuries in HSV1-infected guinea pigs was commensurate to that of 5% acyclovir-based ointment. The virus-containing inepidermic material was rubbed into dehaired scarified zones ($\sim$5 cm^2 each) 48 h after the appearance of the first hyperemic symptoms. The ointment was applied two times a day for five days. In the control group, specific symptomatology (herpetic skin rash) appeared on day 5 after infection and was especially well pronounced by day 10. Complete recovery occurred on day 12.

The therapeutic effect was the most apparent after application of 15Lys-bis-Nt and Lys-bis-Nt in the form of .15% ointment. The size of the injured zone diminished by $\sim$9 and 7%, respectively. The areas affected by vesicular herpetic rash decreased in size reliably in comparison with control. Complete re-epithelization occurred 24 h earlier than in the control group. By comparison, a similar therapeutic effect could be attained through application of acyclovir in the form of 5% ointment with a 30 times higher drug content (by weight) (Andronova et al., 2013). A comparison of *in vivo* effects of two bis-netropsins and acyclovir demonstrated that Lys-bis-Nt and 15Lys-bis-Nt used as ointment-based drugs had much greater curative effects on herpetic infection than acyclovir. The data obtained also show that dimeric derivatives of netropsin serve as effective inhibitors of infections transmitted by acyclovir-resistant HSV1 strains in cases where oral or intraepidermic administration of acyclovir has little effect.

Acknowledgments

This work has been carried out with the financial support of the Program of the Presidium of the Russian Academy of Sciences for Molecular and Cellular Biology and the Russian Foundation for Basic Research (Grant No. 11-04-02001). The valuable assistance of Dr. A.B. Poltaraus and coworkers in sequencing cloned DNA fragments is highly appreciated.

References

Andronova, V. L., Grokhovsky, S. L., Deryabin, P. G., Gursky, G. V., Galegov, G. A., & L'vov, D. K. (2012). Antiherpetic activity of netropsin derivatives as tested in experiments on laboratory animals. *Voprosi Virusologii (Russian), 57*, 24–26.

Andronova, V. L., Grokhovsky, S. L., Surovaya, A. N., Arkhipova, V. S., Gursky, G. V., & Galegov, G. A. (2008). Antiviral and cytotoxic activity of netropsin derivatives in Vero cells infected with vaccinia virus and herpes simplex virus type I. *Doklady Biochemistry and Biophysics, 422*, 688–693.

Andronova, V. L., Grokhovsky, S. L., Surovaya, A. N., Gursky, G. V., & Galegov, G. A. (2001). Antiherpetic activity of dimeric derivatives of netropsin. *Doklady Biochemistry and Biophysics, 380*, 345–348.

Andronova, V. L., Grokhovsky, S. L., Surovaya, A. N., Gursky, G. V., & Galegov, G. A. (2004). DNA-binding and antiviral activity of bis-netropsins containing clusters of lysine residues in the N-terminal region. *Doklady Biochemistry and Biophysics, 399*, 829–834.

Andronova, V. L., Grokhovsky, S. L., Surovaya, A. N., Gursky, G. V., & Galegov, G. A. (2007). Effect of dimeric derivatives of netropsin and their combinations with acyclovir on herpes simplex virus type 1 infection in mice. *Doklady Biochemistry and Biophysics, 413*, 830–834.

Andronova, V. L., Grokhovsky, S. L., Surovaya, A. N., Gursky, G. V., & Galegov, G. A. (2013). Estimation of the activities of bis-netropsin derivatives on a model of an experimental cutaneous herpes simplex disease of guinea pigs. *Voprosi Virusologii (Russian), 58*, 32–35.

Ariyoshi, M., Nishino, T., Iwasaki, H., Shinagawa, H., & Morikawa, K. (2000). Crystal structure of the Holliday junction DNA in complex with a single RuvA tetramer. *Proceedings of the National Academy of Sciences of the USA, 97*, 8257–8262.

Aslani, A., Macao, B., Simonsson, S., & Elias, P. (2001). Complementary intrastrand base pairing during initiation of herpes simplex virus type 1 DNA replication. *Proceedings of the National Academy of Sciences of the USA, 98*, 7194–7199.

Aslani, A., Olsson, M., & Elias, P. (2002). ATP-dependent unwinding of a minimal origin of DNA replication by the origin-binding protein and the single-strand DNA-binding protein ICP8 from herpes simplex virus type I. *Journal of Biological Chemistry, 277*, 41204–41212.

Bailly, C., & Chaires, J. B. (1998). Sequence-specific DNA minor groove binders: Design and synthesis of netropsin and distamycin analogues. *Bioconjugate Chemistry, 9*, 513–538.

Bazhulina, N. P., Surovaya, A. N., Gursky, Y. G., Andronova, V. L., Arkhipova, V. S., Golovkin, M. V., … Gursky, G. V. (2012). Inhibition of herpes simplex virus helicase UL9 by netropsin derivatives and antiviral activities of bis-netropsins. *Biophysics, 57*, 153–162.

Belikov, S. L., Grokhovsky, S. L., Isaguliants, M. G., Surovaya, A. N., & Gursky, G. V. (2005). Sequence-specific minor groove binding ligands as potential regulators of gene expression in *Xenopus Laevis* oocytes. *Journal of Biomolecular Structure & Dynamics, 23*, 193–202.

Belon, C. A., High, Y. D., Lin, T. I., Pauwells, F., & Frick, D. N. (2010). Mechanism and specificity of a symmetrical benzimidazolephenylcarboxamide helicase inhibitor. *Biochemistry, 49*, 1822–1832.

Bennett, R. J., & West, S. C. (1995). RuvC protein resolves Holliday junctions via cleavage of the continuous (non-crossover) strands. *Proceedings of the National Academy of Sciences of the USA, 92*, 5635–5639.

Biertümpfel, C., Yang, W., & Suck, D. (2007). Crystal structure of T4 endonuclease VII resolving a Holliday junction. *Nature, 449*, 616–620.

Boehmer, P. E., Craigie, M. C., Stow, N. D., & Lehman, I. R. (1994). Association of origin binding protein and single strand DNA-binding protein, ICP8, during herpes simplex virus type 1 DNA replication *in vivo*. *Journal of Biological Chemistry, 269*, 29329–29334.

Carter, A. S., Tahmaseb, K., Compton, S. A., & Matson, S. W. (2012). Resolving Holliday junctions with *Escherichia coli* UvrD helicase. *Journal of Biological Chemistry, 287*, 8126–8134.

Chattopadhyay, S., & Weller, S. K. (2007). Direct interaction between the N- and C-terminal portions of the herpes simplex virus type 1 origin binding protein UL9 implies the formation of a head-to-tail dimer. *Journal of Virology, 81*, 13659–13667.

Chen, X., Ramakrishnan, B., Rao, S. T., & Sundaralingam, M. (1994). Binding of two distamycin A molecules in the minor groove of an alternating B-DNA duplex. *Structural Biology, 1*, 169–175.

Coll, M., Frederick, C. A., Wang, A. H.-J., & Rich, A. (1987). A bifurcated hydrogen bonded conformation in the d(AT) base pairs of the DNA dodecamer d(CGCAAATTTGCG) and its complex with distamycin. *Proceedings of the National Academy of Sciences of the USA, 84*, 8385–8389.

Coull, J. J., He, G., Melander, Ch., Rucker, V. C., Dervan, P. B., & Margolis, D. M. (2002). Targeted derepression of the human immunodeficiency virus type 1 long terminal repeat by pyrrole-imidazole polyamides. *Journal of Virology, 76*, 12349–12354.

Dickinson, L. A., Gulizia, R. J., Trauger, J. W., Baird, E. E., Mosier, D. E., Gottesfeld, J. M., & Dervan, P. B. (1998). Inhibition of RNA polymerase II transcription in human cells by synthetic DNA-binding ligands. *Proceedings of the National Academy of Sciences of the USA, 95*, 12890–12895.

Doherty, A. J., Serpell, L. C., & Ponting, Ch. P. (1996). The helix–hairpin–helix DNA-binding motif: A structural basis for non-sequence-specific recognition of DNA. *Nucleic Acids Research, 24*, 2488–2492.

Fierer, D. S., & Challberg, M. D. (1992). Purification and characterization of UL9, the herpes simplex virus type 1 origin-binding protein. *Journal of Virology, 66*, 3986–3995.

Förster, Th. (1948). Intermolecular energy migration and fluorescence. *Annalen der Physik, 2*, 55–75.

Gearhart, M. D., Dickinson, L., Ehley, J., Melander, Ch., Dervan, P. B., Wright, P. E., & Gottesfel, J. L. (2005). Inhibition of DNA binding by human estrogen-related receptor 2 and estrogen receptor α with minor groove binding polyamides. *Biochemistry, 44*, 4196–4203.

Geierstanger, B. H., Mrksich, M., Dervan, P. B., & Wemmer, D. E. (1994). Design of a G•C-specific DNA minor groove-binding peptide. *Science, 266*, 646–650.

Gopal, D. N., Guo, F., & Van Duyne, G. D. (1998). Structure of the Holliday junction intermediate in *Cre-loxP* site-specific recombination. *The EMBO Journal, 17*, 4175–4187.

Grokhovsky, S. L., Gottikh, B. P., & Zhuze, A. L. (1992). Ligands possessing affinity to specific DNA base pair sequences. IX. Synthesis of netropsin and distamycin A analogs having sarcolysine residues or a platinum(II) atom. *Bioorganic Chemistry, 18*, 570–583.

Grokhovsky, S. L., Nikolaev, V. A., Zubarev, V. E., Surovaya, A. N., Zhuze, A. L., Chernov, B. K., … Gursky, G. V. (1993). Specific DNA cleavage by a netropsin analog containing a copper(II)-chelating peptide Gly-Gly-His. *Molecular Biology, 6*, 839–850.

Grokhovsky, S. L., Surovaya, A. N., Burckhardt, G., Pismensky, V. F., Chernov, B. K., Zimmer, C., & Gursky, G. V. (1998). DNA sequence recognition by bis-linked netropsin and distamycin derivatives. *FEBS Letters, 439*, 346–350.

Grokhovsky, S. L., Surovaya, A. N., Sidorova, N. Yu., Votavova, H., Sponar, J., Frich, I., & Gursky, G. V. (1988). Design and synthesis of peptides capable of binding specically to DNA. *Molecular Biology, 22*, 1056–1073.

Gursky, G. V., Nikitin, A. M., Surovaya, A. N., Grokhovsky, S. L., Andronova, V. L., Galegov. G. A. (2008). *Isohelical DNA-binding oligomers: Antiviral activity and application for design of nano-structured devices. Nanomaterials for Application in Medicine and Biology* (*NATO Workshop: Security through Science Series C: Environmental Security, Bonn*) (pp. 17–28). Dordrecht: Springer.

Gursky, G. V., Zasedatelev, A. S., Zhuze, A. L., Khorlin, A. A., Grokhovsky, S. L., Streltsov, S. A., … Gottikh, B. P. (1983). Synthetic sequence-specific ligands. *Cold Spring Harbor Symposium Quantitative Biology, 47*, 367–378.

Hadden, J. M., Déclais, A. C., Carr, S. B., Lilley, D. M., & Phillips, S. E. (2007). The structural basis of Holliday junction resolution by T7 endonuclease I. *Nature, 449*, 621–624.

He, X., & Lehman, I. R. (2001). An initial ATP-independent step in the unwinding of a herpes simplex virus type I origin of replication by a complex of the viral origin-binding protein and single-strand DNA-binding protein. *Proceedings of the National Academy of Sciences of the USA, 98*, 3024–3028.

Janssen, S., Cuvier, O., Muller, M., & Laemmli, U. K. (2000). Specific gain- and loss-of-function phenotypes induced by satellite-specific DNA-binding drugs fed to Drosophila melanogaster. *Molecular Cell, 6*, 1013–1024.

Khorlin, A. A., Krylov, A. S., Grokhovsky, S. L., Zhuze, A. L., Zasedatelev, A. S., Gursky, G. V., & Gottikh, B. P. (1980). A new type of AT-specific ligand constructed of two netropsin-like molecules. *FEBS Letters, 118*, 311–314.

Kleikopf, C. L., Bremer, R. E., White, S., Szewczyk, J. W., Turner, J. M., Baird, E. E., … Rees, D. C. (2000). Structural effects of DNA sequence on TA recognition by hydroxypyrrole/pyrrole pairs in the minor groove. *Journal of Molecular Biology, 295*, 557–567.

Klevit, R. E., Wemmer, D. E., & Reid, B. R. (1986). 1H NMR studies on the interaction between distamycin A and a symmetrical DNA dodecamer. *Biochemistry, 25*, 3296–3303.

Koff, A., Schwedes, J. F., & Tegtmeyer, P. J. (1991). Herpes simplex virus origin-binding protein (UL9) loops and distorts the viral replication origin. *Journal of Virology, 65*, 3284–3292.

Kopka, M. L., Goodsell, D. S., Han, G. W., Chiu, T. K., Lown, J. W., & Dickerson, R. E. (1997). Defining GC-specificity in the minor groove: Side-by-side binding of diimidazole lexitropsin to CATGGCCATG. *Structure, 5*, 1033–1044.

Kopka, M. L., Yoon, C., Goodsell, D., Pjura, P., & Dickerson, R. E. (1985). The molecular origin of DNA-drug specificity in netropsin and distamycin. *Proceedings of the National Academy of Sciences of the USA, 82*, 1376–1380.

Lee, S. S., & Lehman, I. R. (1997). Unwinding of the box I element of a herpes simplex virus type 1 origin by a complex of the viral origin binding protein, single-strand DNA binding protein, and single-stranded DNA. *Proceedings of the National Academy of Sciences of the USA, 94*, 2838–2842.

Leinsoo, T. A., Nikolaev, V. A., Grokhovsky, S. L., Strel'tsov, S. A., Zasedatelev, A. S., Zhuze, A. L., & Gursky, G. V. (1988). Attachment of trivaline to a netropsin analog changes the specificity of its binding to DNA. *Molecular Biology, 22*, 159–175.

Lown, J. W., Krowicki, K., Balzarini, J., Newman, R. A., & De Clerk, E. (1989). Novel linked antiviral and antitumor agents related to netropsin and distamycin: Synthesis and biological evaluation. *Journal of Medical Chemistry, 32*, 2368–2375.

Macao, B., Olsson, M., & Elias, P. (2004). Functional properties of the herpes simplex virus type I origin-binding protein are controlled by precise interactions with the activated form of the origin of DNA replication. *Journal of Biological Chemistry, 279*, 29211–29217.

Mahdi, A. A., McGlynn, P., Levett, S. D., & Lloyd, R. G. (1997). DNA binding and helicase domains of the *Escherichia coli* recombination protein RecG. *Nucleic Acids Research, 25*, 3875–3880.

Makhov, A. M., Boehmer, P. E., Lehman, I. R., & Griffith, J. D. (1996). The herpes simplex virus type 1 origin-binding protein carries out origin specific DNA unwinding and forms stem-loop structures. *EMBO Journal, 15*, 1742–1750.

Malik, A. K., & Weller, S. K. (1996). Use of transdominant mutants of the origin-binding protein (UL9) of herpes simplex virus type 1 to define functional domains. *Journal of Virology, 70*, 7859–7866.

Manolaridis, I., Mumtsidu, E., Konarev, P., Makhov, A. M., Fullerton, S. W., Sinz, A., … Tucker, P. A. (2009). Structural and biophysical characterization of the proteins interacting with the herpes simplex virus 1 origin of replication. *Journal of Biological Chemistry, 284*, 16343–16353.

Marras, S. A. E., Kramer, F. R., & Tyagi, S. (2002). Efficiencies of fluorescence resonance energy transfer and contact-mediated quenching in oligonucleotide probes. *Nucleic Acids Research, 30*, e122.

Meier, J. L., Montgomery, D. C., & Dervan, P. B. (2012). Enhancing the cellular uptake of Py-Im polyamides through next generation aryl turns. *Nucleic Acids Research, 40*, 2345–2356.

Moiseeva, E. D., Bazhulina, N. P., Gursky, Y. G., Surovaya, A. N., Grokhovsky, S. L., & Gursky G. V. (2013). DNA helicase UL9 of herpes simplex virus type 1 binds to the synthetic 4-ways Holiday junction and unwinds it in the presence of ATP. *Doklady Biochemistry and Biophysics, 450*.

Mrksich, M., Parks, M. E., & Dervan, P. B. (1994). Hairpin peptide motif: A new class of oligopeptides for sequence-specific recognition in the minor groove of double-helical DNA. *Journal of American Chemical Society, 116*, 7983–7988.

Nikolaev, V. A., Grokhovsky, S. L., Surovaya, A. N., Leinsoo, T. A., Sidorova, N. Yu., Zasedatelev, A. S., … Gursky, G. V. (1996). Design of sequence-specific DNA binding ligands that use a two-stranded peptide motif for DNA sequence recognition. *Journal of Biomolecular Structure & Dynamics, 14*, 31–47.

Nishino, T., Ariyoshi, M., Iwasaki, H., Shinagawa, H., & Morikawa, K. (1998). Functional analyses of the domain structure in the Holliday junction binding protein RuvA. *Structure, 6*, 11–21.

Olsson, M., Tang, Ka-W, Persson, C., Wilhelmsson, L. M., Billeter, M., & Elias, P. (2009). Stepwise evolution of the herpes simplex virus origin binding protein and origin of replication. *Journal of Biological Chemistry, 284*, 16246–16255.

Ortiz-Lombardia, M., Gonzalez, A., Eritja, R., Aymami, J., Azorin, F., & Coll, M. (1999). Crystal structure of a DNA Holliday junction. *Nature Structural Biology, 6*, 913–917.

Pelton, J. G., & Wemmer, D. E. (1989). Structural characterization of a 2:1 distamycin A d(CGCAAATTGGC) complex by two-dimensional NMR. *Proceedings of the National Academy of Sciences of the USA, 86*, 5723–5727.

Rafferty, J. B., Sedelnikova, S. E., Hargreaves, D., Artymiuk, P. J., Baker, P. J., Sharples, G. J., … Rice, D. W. (1996). Crystal structure of DNA recombination protein RuvA and a model for its binding to the Holliday junction. *Science, 274*, 415–421.

Sambrook, J., Fritsch, E. F., & Maniatis, T. (1989). *Molecular cloning: A laboratory manual*. Cold Spring Harbor, NY: Cold Spring Harbor Laboratory Press.

Shao, X., & Grishin, N. V. (2000). Common fold in helix-hairpin-helix proteins. *Nucleic Acids Research, 28*, 2643–2650.

Surovaya, A. N., Grokhovsky, S. L., Bazhulina, N. P., & Gursky, G. V. (2008). DNA-binding activity of bis-netropsins containing a *cis*-diaminoplatinum group between two netropsin fragments. *Biophysics, 53*, 744–753.

Surovaya, A. N., Grokhovsky, S. L., Brusov, R. V., Lysov, Yu. P., Zhuze, A. L., & Gursky, G. V. (1995). Design of *de novo* DNA-binding peptides with β-strand-turn-β-strand motif for DNA sequence recognition. *Molecular Biology, 28*, 859–868.

Surovaya, A. N., Grokhovsky, S. L., Gursky, Ya. G., Andronova, V. L., Arkhipova, V. S., Bazhulina, N. P., … Gursky, G. V. (2010). Complex of the herpes simplex virus initiator protein UL9 with DNA as a platform for the design of a new type of antiviral drugs. *Biophysics, 55*, 206–216.

Weir, H. M., & Stow, N. D. (1990). Two binding sites for the herpes simplex virus type 1 UL9 protein are required for efficient activity of the OriS replication origin. *Journal of General Virology, 71*, 1379–1385.

Whitby, M. C., & Lloyd, R. C. (1998). Targeting Holliday junctions by the RecG branch migration protein of *Escherichia coli*. *Journal of Biological Chemistry, 273*, 19729–19739.

White, S., Szewczyk, J. W., Turner, J. M., Baird, E. E., & Dervan, P. B. (1998). Recognition of the four Watson-Crick base pairs in the DNA minor groove by synthetic ligands. *Nature, 391*, 468–471.